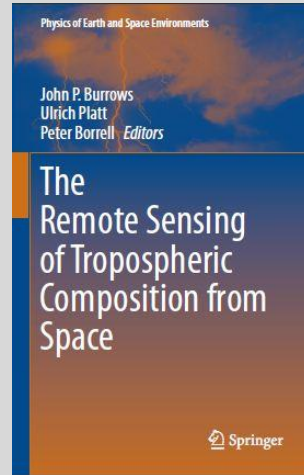


# **The Remote Sensing of Tropospheric Composition from Space**

Editors:

John P. Burrows  
Ulrich Platt  
Peter Borrell

*Pages 315 to 364*



## **Chapter 7**

### **Data Quality and Validation of Satellite Measurements of Tropospheric Composition**

Ankie J.M. Peters, Brigitte Buchmann, Dominik  
Brunner, Ronald C. Cohen, Jean-Christopher  
Lambert, Gerrit de Leeuw, Piet Stammes,  
Michiel van Weele and Folkard Wittrock

Publisher: Springer Verlag, Heidelberg

[Springer Book Web Page](#)

[Springer on line Page for the Book](#)

ISBN 978-3-642-14790-6

DOI 10.1007/978-3-642-14791-3

**February 2011**



# Chapter 7

## Data Quality and Validation of Satellite Measurements of Tropospheric Composition

Ankie J.M. Pipers, Brigitte Buchmann, Dominik Brunner, Ronald C. Cohen, Jean-Christopher Lambert, Gerrit de Leeuw, Piet Stammes, Michiel van Weele and Folkard Wittrock

### 7.1 Introduction

When using satellite tropospheric products for atmospheric research and monitoring or for other applications (see Chapters 8 and 9), it is essential to understand their significance. It is therefore important to take into account appropriate estimates of their uncertainties and to understand their capabilities and limitations. Some central questions are listed. How representative are the satellite retrieved products for the actual atmospheric state? Is there a bias and uncertainty with respect to the “truth”? How deep can satellites measure into the boundary layer? How well do they capture temporal variations of atmospheric composition, from daily fluctuations to decadal trends? How well do they capture spatial structures, from local emission sources to global features? It is important to realise that the answers to these questions depend considerably on the atmospheric situation (e.g. cloudy or clear-sky and polluted or clean situations), knowledge of ancillary parameters (e.g. surface elevation and

---

A.J.M. Pipers (✉), P. Stammes and M. van Weele  
Royal Netherlands Meteorological Institute (KNMI), De Bilt, The Netherlands

B. Buchmann and D. Brunner  
Laboratory for Air Pollution Technology, Empa, Swiss Federal Laboratories for Materials Testing and Research, Dübendorf, Switzerland

R.C. Cohen  
Department of Chemistry, University of California, Berkeley, CA, USA

J.-C. Lambert  
Belgian Institute for Space Aeronomy(BIRA-IASB), Brussels, Belgium

G. de Leeuw  
Climate Change Unit, Finnish Meteorological Institute, Helsinki, Finland  
and  
Department of Physics, Univeristy of Helsinki, Helsinki, Finland  
and  
TNO Environment and Geosciences, Utrecht, The Netherlands

F. Wittrock  
Institute of Environmental Physics, University of Bremen, Germany

reflection, as well as the knowledge of instrumental characteristics and viewing geometries (e.g. high sun elevation versus twilight, and instrument noise which depends on the orbital positions, enhanced noise being typical in the South Atlantic Anomaly).

In part these questions can be answered by “validating” the satellite data, see definitions in Section 7.2.1. A major goal of validation is to describe and to quantify the uncertainty of a satellite product in such a way that it is of direct use for the specific expected research or application areas, in other words to assess its fitness-for-purpose. Another goal is to test and confirm the theoretical error budget of satellite data derived from algorithm sensitivity studies. Table 7.1 lists the estimated current uncertainties of some relevant tropospheric satellite products and the main source of validation measurements.

Usually validation is based on comparisons with independent measurements of the same parameter with known uncertainties. When comparing satellite data to correlative measurements or to modelling results, differences in observed air mass and in observation, and retrieval techniques, have to be taken into account. A summary of the different methods of comparing two data sets, including the use of models is given in Section 7.2. In addition, the methods used for verification and monitoring of quality parameters are also described. The validation of tropospheric satellite products is a relatively young field, and the methods described in Section 7.2 are expected to develop and evolve as tropospheric research with satellite data develops.

Section 7.3 addresses various aspects of quality assurance, which starts before launch and is included in the mission planning and continues during satellite life time.

Validation measurements have, typically, to be performed for a wide range of possible values and for different atmospheric and measurement conditions. Comparison methods have to consider appropriate differences in spatial and temporal resolution and sampling, especially in the presence of significant spatial structures and temporal variations of the species. It is essential that the correlative measurements and validation studies provide the necessary knowledge of all parameters affecting the measurement and the retrieval algorithm (e.g. surface albedo, cloud fraction) and the relevant ranges of the parameters that might have an impact on the uncertainty (see Chapters 2, 3 and 4).

Section 7.4 provides a more comprehensive understanding of the characteristic differences of the various tropospheric species, which have a direct impact on the validation strategy: where, when and how to perform validation measurements and carry out comparisons. The distribution and variability of the tropospheric species are discussed as well as the relevant and significant atmospheric processes. In Section 7.4, we discuss further what measurements are needed to investigate and verify the sensitivities of retrievals, to key parameters such as clouds, albedo and aerosol.

Several measurement techniques are currently used for the validation of tropospheric satellite data products. Section 7.5 details their main characteristics. Most

**Table 7.1** Estimated uncertainties of some of the relevant tropospheric satellite products and the main source of validation measurements. Uncertainties will vary for different instruments and situations. Values given here are from the quoted references

Troposp. satellite product	Tropospheric lifetime <sup>a</sup>	Satellite instrument	Dominant validation source	Estimated current best uncertainty	References	Note
NO <sub>2</sub>	h to d <sup>b</sup>	GOME	MAXDOAS/ aircraft	30–50%	Celarier et al. (2008), Brinksma et al. (2008), Bucseia et al. (2008)	
		SCIAMACHY				
		OMI				
		GOME-2				
O <sub>3</sub>	h to d <sup>b</sup>	TES	O <sub>3</sub> sondes	20–30%	Nassar et al. (2008)	
		GOME				
		SCIAMACHY				
		OMI				
		GOME-2				
		TES				
CO	2 mt	IASI	FTIR	20–30%	Dils et al. (2006)	5% in monthly mean
		AIRS				
		MOPITT				
		SCIAMACHY				
		AIRS				
		TES				
		IASI				
		GOME				
		SCIAMACHY				
		OMI				
HCHO	h to d <sup>c</sup>	GOME-2	MAXDOAS	20–50%	De Smedt et al. (2008)	
		SCIAMACHY				
		OMI				
		GOME-2				
		SCIAMACHY				
		OMI				
CHOCHO	h to d <sup>c</sup>	GOME-2	MAXDOAS	30–50%	Wittrock et al. (2006)	In monthly mean
		SCIAMACHY				
		OMI				
CH <sub>4</sub>	12 y	GOME-2	FTIR	1–2%	Dils et al. (2006)	
		SCIAMACHY				
		AIRS				
		TES				
		IASI				

*(continued)*

Table 7.1 (continued)

Troposp. satellite product	Tropospheric lifetime <sup>a</sup>	Satellite instrument	Dominant validation source	Estimated current best uncertainty	References	Note
SO <sub>2</sub>	h	GOME SCIAMACHY OMI	Aircraft	1.5 DU	Krotkov et al. (2008)	
BrO	m	GOME-2 GOME SCIAMACHY OMI	–	–		
H <sub>2</sub> O	–	GOME-2 GOME SCIAMACHY GOME-2 AIRS TES	SSM/I	0.1–0.2 g/cm <sup>2</sup>	Noel et al. (2005)	In daily mean
CO <sub>2</sub>	100 y	IASI SCIAMACHY GOSAT	FTIR	5%	Dils et al. (2006)	In monthly mean
N <sub>2</sub> O	114 y	TES SCIAMACHY TES IASI	FTIR	10%	Dils et al. (2006)	
Aerosol Optical Depth	up to a week	IASI <sup>d</sup>	Sun-photometer (AERONET)	±0.05±0.15τ	Remer et al. (2005)	Over land

<sup>a</sup>average life times (or ranges) in the troposphere; *m* minutes, *h* hours, *d* days, *mt* months, *y* years

<sup>b</sup>lower to upper troposphere

<sup>c</sup>depending on latitude (radiation)

<sup>d</sup>Aerosol Optical Depth and many other aerosol properties are retrieved from: POLDER, MODIS, CALIPSO, AVHRR, SeaWiFS, MERIS, MISR, SEVIRI, AATSR, GOME, SCIAMACHY, OMI and GOME-2., see Chapter 6 for details

of the existing instruments contribute to international networks and data centres, of which examples are given.

Recommendations for future validation strategies are given in Section 7.6.

## 7.2 Methods of Validation

The basis for investigating the quality of satellite data is comparing them to reference data obtained independently and of known quality. The source of the reference data may be from ground-based, air-borne and balloon-borne measurements. In addition, satellite measurements and model output can provide valuable comparisons to help to understand the quality of the satellite data.

The most common methodology for comparing two independent data sets is the comparison of columns and profiles, which are coincident in both time and space. This typically yields an average difference and a spread, which are propagated to estimate for the bias and the uncertainty in the satellite data, provided that those from the reference data are themselves well known.

In the next subsections it is shown that a simple direct comparison as sketched above is often insufficient for the validation of satellite data, and that more sophisticated approaches are needed to characterise the quality of different aspects of the data.

### 7.2.1 Definitions

The process of assessing the quality of satellite data products involves at least the following aspects: validation, verification, calibration and monitoring.

*Validation* is defined by the Committee on Earth Observation Satellites (CEOS) as the process of assessing, by independent means, the quality of the data products derived from the system outputs. The ISO guide of metrology vocabulary (VIM) (ISO 2007) further defines *validation* as verification where the specified requirements are adequate for an intended use. Validation therefore addresses the fitness-for-purpose of the data products via comparisons.

Verification is defined as the provision of objective evidence that a given data product fulfils specified requirements. Data products are checked for internal consistency, out-of-bound values, geographical distribution, and statistical behaviour. The comparison of retrieval methods and the comparison of experimental data with that from models are also called verification. Verification identifies errors in the retrieval software or auxiliary data. Validation and verification help to optimise the retrieval algorithms.

*Calibration* is defined as the process of quantitatively defining the system responses to known, controlled signal inputs (CEOS). It includes routinely checking the quality of the measured reflectance or transmittance with respect to possible changes in instrument behaviour. Applied calibration functions usually take changes of the instrument into account.

*Monitoring* is the process of routine analysis of specific quality parameters to detect instrumental, processor or auxiliary data problems.

Validation should result in an estimate of the bias and the uncertainty. The ISO guide 99 Vocabulary for International Metrology (VIM) (ISO 2007) defines the *bias* as the systematic error of indication of a measuring system, and the *uncertainty* as the parameter that characterises the dispersion of the values that are being attributed to a measured quantity, based on the information used. The bias therefore is a measure of the total systematic errors, and the uncertainty of the total random errors.

Validation of a data product results in an estimate of the bias and the uncertainty, which may depend on geographical, algorithm and instrumental parameters.

## 7.2.2 Comparing Data Sets

The comparison of two data sets usually comprises the following: the finding of suitable collocations between data sets, the selection and filtering of data, the treatment of the data, and the analysis of the data values and their differences.

### a Finding Collocated Data

The most common way to find collocations is to collect all data within an arbitrary temporal and spatial coincident window spanning, typically, from 200 to 1,000 km and from 1 h to 2 days. The presumed advantage of such a selection window is that the variability caused by differences in air mass is reduced. In Section 7.4.1, the tropospheric processes that underlie this variability are discussed. As expected, this approach works satisfactorily for long-lived species having negligible variability in space and in time, and for which the retrieval has a moderate sensitivity to the vertical structure. When atmospheric variability increases, differences in smoothing and sensitivity result in an increase in the comparison noise. In this context, significant effects, including systematic biases, have been identified for short-lived species, like NO<sub>2</sub> and BrO (e.g. Schaub et al. 2007).

The effective location of a remote sensing measurement can be quite distant from the location of the instrument itself and from the location the instrument is pointing to.

The reason for this is that all remote sensing instruments make use of the absorption, emission or scattering of light by the atmospheric constituent to be measured. Passive instruments measure direct or scattered light from the sun or another light source. Active instruments measure their own scattered light. Absorption, emission or scattering along the path the light has travelled from the light source to the instrument is accumulated. The effective location and extent of these measurements can be calculated using a radiative transfer and atmosphere model.

Therefore, collocation criteria should be applied to the effective locations of the measurements rather than to the locations of the instrument or the location the instrument is pointing to.

The effective horizontal location of profiles measured from a balloon or aircraft is often determined by taking the average location over a relevant altitude range. Emmons et al. (2009), for instance, determine an effective location of aircraft profiles of carbon monoxide, CO, to be compared to MOPITT profiles as the average profile between 500 and 800 hPa, the range where MOPITT has its highest sensitivity.

For long-lived species, the number of collocations can be enhanced using air mass trajectory calculations. In this case, one assumes that the same air mass will be observed at every point along the trajectory.

## b Selection and Filtering

The selected data sets for comparison are prepared by filtering the data according to known quality parameters. These quality parameters are usually documented in product description documents or data “disclaimers”. Filtering is performed on quality flags, error bars, solar zenith angle values, cloud cover values, temperature values, surface albedo, terrain variability, etc. Historical verification and validation analysis may point to certain low-quality data as well. Nassar et al. (2008), for instance, describe how ARM-SGP ozone-sonde measurements have been critical in identifying erroneous TES retrievals that can sometimes result when the lowest layers of the atmosphere are in emission (Fig. 7.1). This finding led to the inclusion of an “emission layer flag” in a subsequent version of the product.

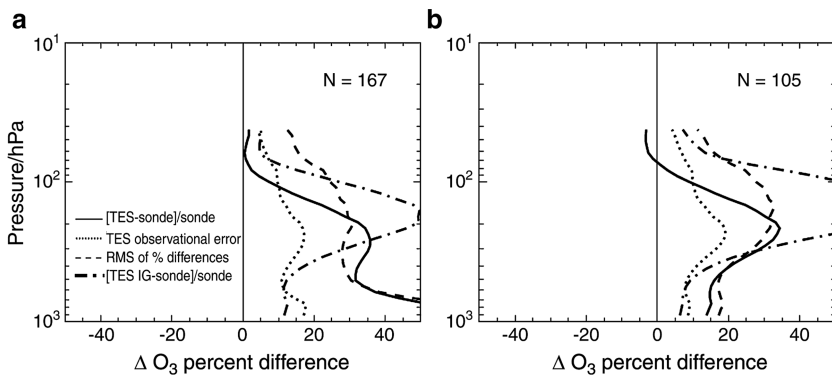


**Fig. 7.1** (a) Average TES-sonde percent difference and RMS for night observations, screened only by the general data quality flag. Note the large values for both average difference and RMS near the surface. (b) Night observations excluding TES scenes with an emission layer identified. IG indicates initial guess. (from Nassar et al. (2008)).

Selection of subsets of data is performed to study the quality of the satellite data for specific situations such as high surface albedo, cloud-free, tropics, or polluted regions. The division in latitude bands or seasons is very common for datasets with several thousands of collocated points. For the validation of TES tropospheric

ozone with ozone sondes, for example, Nassar et al. (2008) found  $\sim 1,600$  collocations in a 2 year data set, so that the comparisons could be performed in 6 latitude bands, with 35–699 collocations in each. The northern mid-latitudes ( $35^\circ$ – $56^\circ$ N) data set with 699 collocations could then be subdivided in data sets for four seasons, with 45–409 collocations in each.

### c Data Treatment

#### Vertical Representation

A tropospheric satellite product is often expressed as a column amount below the tropopause or, in the case of profiles, as partial columns in discrete layers or as number densities at discrete altitudes. However, the retrieved values are generally sensitive to variations at other altitudes as well. The *averaging kernel* (Chapter 2) describes the sensitivity of the retrieved values to the actual values at different altitudes. It is a measure for the vertical resolution of the retrieved profiles or, in the case of tropospheric columns, for the sensitivity to, for example, the boundary layer. When comparing satellite products with correlative data, differences in vertical sensitivity between these data sets have to be taken into account, for example by using the averaging kernel information.

Methods for comparing profiles with different degrees of vertical smoothing are described by Rodgers and Connor (2003) and Calisesi et al. (2005). From these methods a bias and uncertainty can be attributed to the satellite retrieved values. These should however not be mistaken as estimates of the deviation from the “true” value, but rather as estimates of the deviation from the expected value based on the “truth” in combination with known retrieval and measurement sensitivities.

An example for the validation of GOME tropospheric nitrogen dioxide,  $\text{NO}_2$ , is given in Fig. 7.2. Schaub et al (2006) made comparisons with ground-based columns deduced from *in situ* measurements at different altitudes in the Alps, both with and without applying averaging kernels. They found a clear improvement of the comparison under cloudy conditions after multiplying with the averaging kernels, which implies larger errors in the *a priori*  $\text{NO}_2$  profiles under cloudy conditions.

Lamsal et al. (2008) constructed ground-level  $\text{NO}_2$  ( $S_O$ ) from OMI tropospheric columns ( $\Omega_O$ ), using the GEOS-CHEM model as interface:

$$S_O = \frac{vS_G\Omega_O}{v\Omega_G + (1-v)\Omega_G^F} \quad (7.1)$$

where  $S_G$  and  $\Omega_G$  are the ground-level and tropospheric  $\text{NO}_2$  from GEOS-CHEM,  $v$  is the ratio of the local OMI tropospheric  $\text{NO}_2$  column over the mean OMI tropospheric  $\text{NO}_2$  column averaged over the GEOS-CHEM grid cell, and  $\Omega_G^F$  is the modelled free tropospheric  $\text{NO}_2$  column (Fig. 7.3).

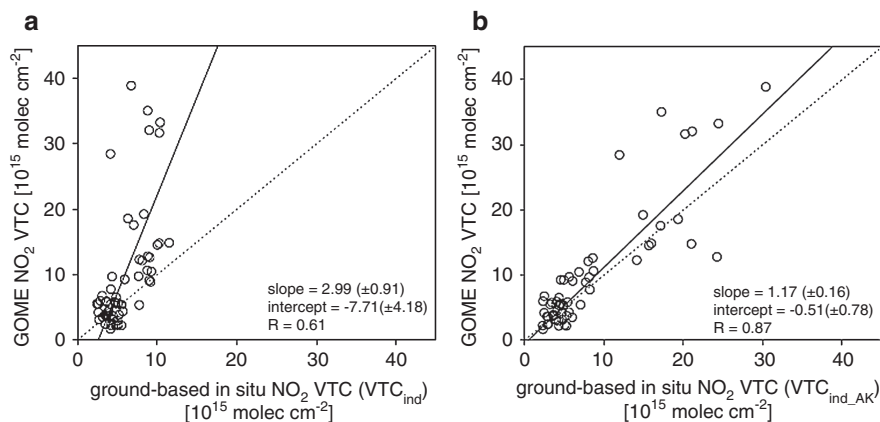


**Fig. 7.2** Comparison between GOME tropospheric  $\text{NO}_2$  columns and those derived from ground-based *in situ* measurements before (a) and after (b) multiplying the ground-based profile with the averaging kernel for cloudy conditions. Columns with  $\text{SCD}_{\text{drop}}/\text{SCD} > 50\%$  are rejected. (from Schaub et al. (2006)).

### Time Differences

For validation of short-lived species like BrO, or  $\text{NO}_2$ , photochemical corrections can be used to account for time differences between the observations. This has been applied successfully for validation of stratospheric columns and profiles (Theys et al. 2006; Dorf et al. 2006), but is not yet common practice for tropospheric product validation. Brinksma et al. (2008) linearly interpolate ground-based MAX-DOAS  $\text{NO}_2$  data to the time of the satellite measurement, which only works if the gaps between the MAX-DOAS measurements are not too large.

Daily averages of FTIR measurements from  $\text{CO}_2$ ,  $\text{CH}_4$ ,  $\text{N}_2\text{O}$ , and CO have been fitted to a third order polynomial in time. The fit-values at the time of satellite measurements have been used to compare with SCIAMACHY values (which are at a given geographic location only available every 6 days) (Sussmann and Buchwitz 2005; Dils et al. 2006), see Fig. 7.4. This only works for rather long-lived and therefore well-mixed species and when the ground-based instrument is far away from variable sources.

### Horizontal Representation

Columns measured from a high-altitude station are typically smaller than the total column measured by a satellite, since the average surface elevation in the satellite pixel is lower than the station altitude. To account for these differences the column amounts can be converted to average volume mixing ratios (Dils et al. 2006). For  $\text{CH}_4$  and CO, Dils et al. (2006) additionally used a modelled scaling factor to

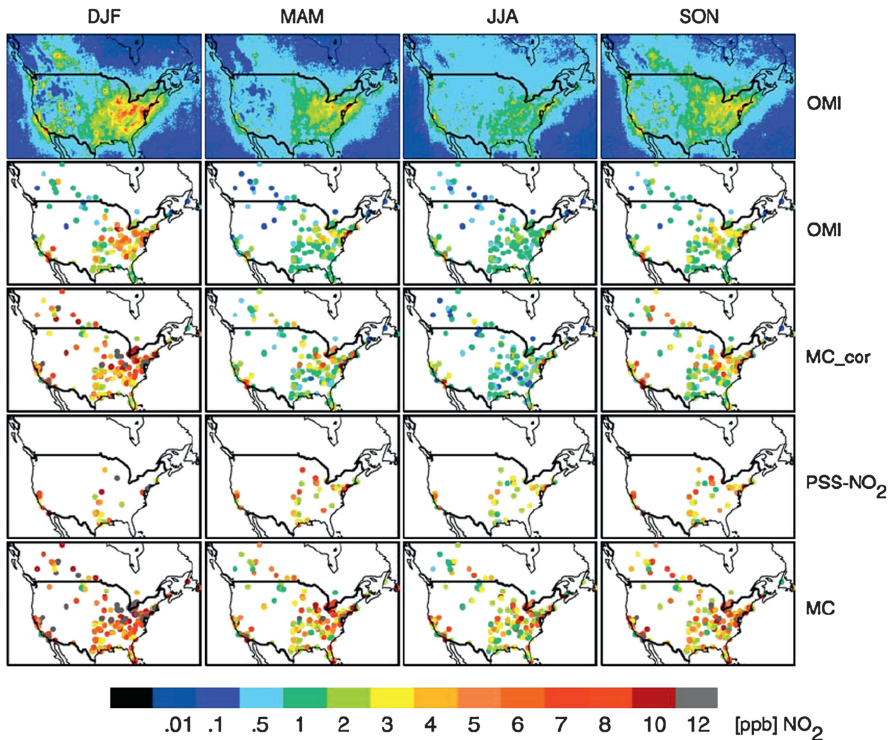


**Fig. 7.3** Seasonal average of surface NO<sub>2</sub> mixing ratios for the year 2005. *First row:* A seasonal map of OMI-derived surface NO<sub>2</sub> over North America. *Second row:* The collocated OMI-derived surface NO<sub>2</sub> at the molybdenum converter *in situ* sites. *Third row:* The corrected molybdenum converter *in situ* measurements. *Fourth row:* Alternative photochemical steady-state calculation of surface NO<sub>2</sub>. *Fifth row:* The molybdenum converter *in situ* measurements. (from Lamsal et al. (2008)).

account for the fact that the volume mixing ratio is not constant as a function of altitude.

To account for spatial inhomogeneity within the tropospheric NO<sub>2</sub> field, Brinkma et al. (2008) averaged MAX-DOAS measurements in three different directions.

Kramer et al. (2008) constructed representative FOV-weighted *in situ* NO<sub>2</sub> measurements  $x'$  for validation of OMI tropospheric NO<sub>2</sub> by weighing the *in situ* NO<sub>2</sub> mixing ratio  $x_u$  from an urban station in Leicester and that from a background station  $x_{bg}$  with the fraction  $a$  of the satellite pixel sampling the Leicester urban area:  $x' = ax_u + (1 - a)x_{bg}$  (Fig. 7.5).

Celarier et al. (2008) constructed representative satellite tropospheric NO<sub>2</sub> measurements for comparison to an MFDOAS by integrating the OMI NO<sub>2</sub> field within the MFDOAS Field of View (Fig. 7.6).

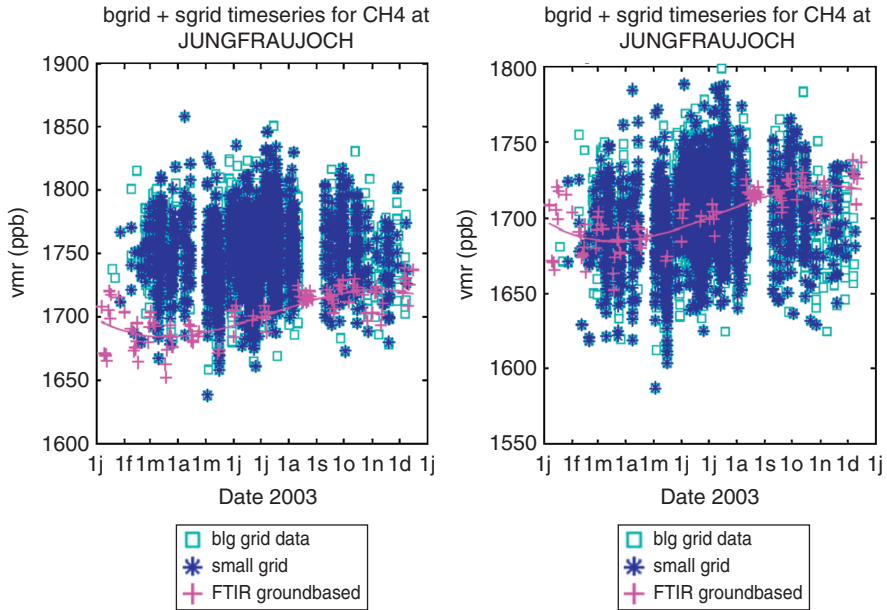


**Fig. 7.4** FTIR data relative to their polynomial fit. Time series of CH<sub>4</sub> measurements at Jungfraujoch from ground-based FTIR (+) and SCIAMACHY IMAP-DOAS (*open squares* for large collocation grid; *stars* for small collocation grid). *Left:* original CH<sub>4</sub> mixing ratios (*open squares* and *stars*) and third order polynomial fit through the ground-based FTIR data (*solid line*). *Right:* CH<sub>4</sub> mixing ratios (*open squares* and *stars*) after the application of a correction factor and third order polynomial fit through the FTIR ground-based data (*solid line*). (from Dils et al. (2006)).

### Noise Reduction

For satellite products with large retrieval uncertainties, it is often not feasible to compare individual measurements. For these products, (weighted) averages in time and space are compared to correlative data. It is important to realise that estimates for the uncertainty of the satellite data product resulting from such a comparison are valid for the averaged products and not for the individual measurements. An example is given in Buchwitz et al. (2007), where SCIAMACHY and MOPITT data are averaged over specific regions before comparing them (see Fig. 7.7).

### d Analysing the Data

The last part of the comparison is the analysis of the data. The data sets can be analysed:

- As function of time: do they have the same temporal behaviour? scatter plot, with correlation coefficient and/or a linear fit.

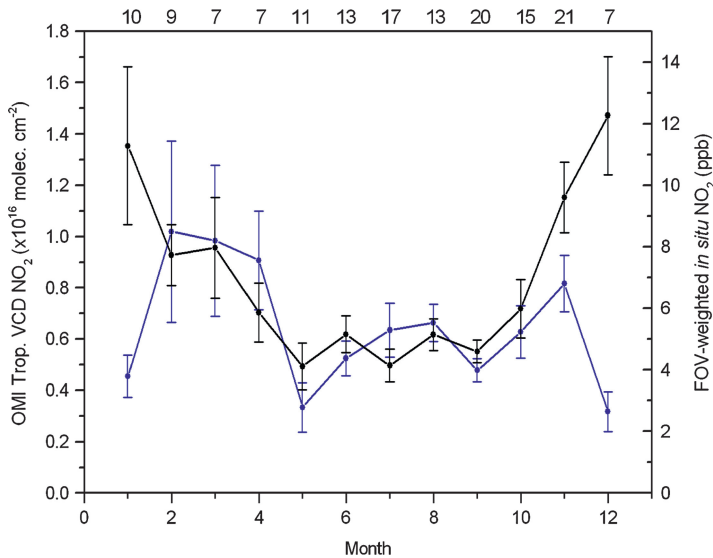


**Fig. 7.5** Monthly averages of NO<sub>2</sub> for 150 cloud-free days (cloud fraction less than 20%) between January 2005 and December 2006 for OMI tropospheric columns (blue) and coincident mean FOV-weighted *in situ* data from Leicester area (black); the error bars show the standard deviation on the mean. The number of cloud-free observations for each month is shown at the top of the plot (from Kramer et al. (2008)).

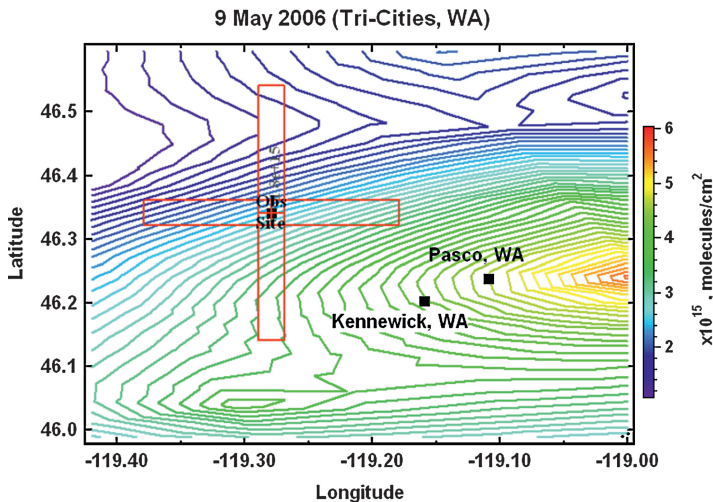


**Fig. 7.6** Tropospheric NO<sub>2</sub> vertical column density over the Tri-Cities area of Washington State on the 9th May 2006. The contour map is derived from the individual OMI FOV measurements. The red rectangles show the tropospheric region viewed by the MF-DOAS instrument. The centers of population for the cities of Kennewick and Pasco are indicated by black squares. (from Celarier et al. (2008)).

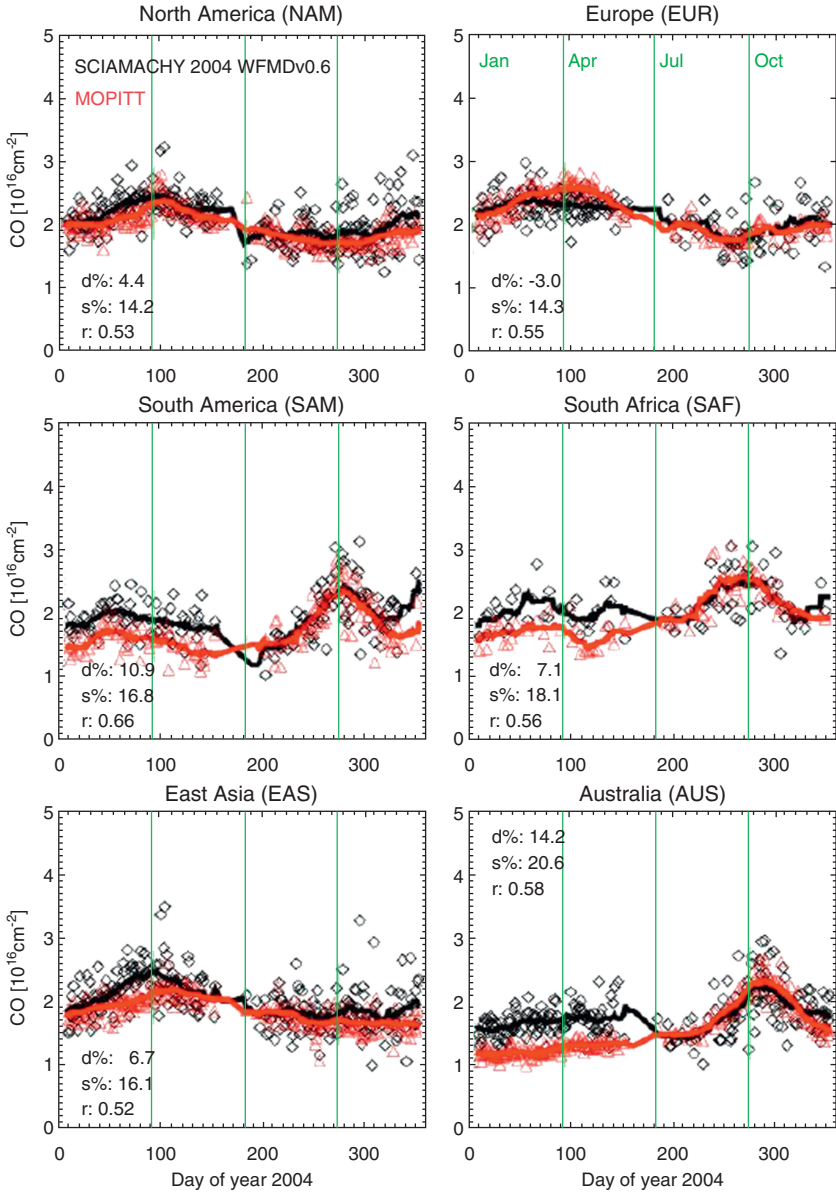


**Fig. 7.7** Regional comparison of SCIAMACHY WFMDv0.6 CO columns (black) with MOPITT (red) for the year 2004. The symbols show the daily averages of all coincident grid points. For SCIAMACHY, all measurements have been averaged for which the WFMDv0.6 quality flag indicates a successful measurement. The solid lines represent 30 day running averages. For each region the following quantities are shown which have been computed based on the unsmoothed daily averages: d% is the mean difference SCIA–MOPITT in percent, s% denotes the standard deviation of the difference in percent, and r is the correlation coefficient. (from Buchwitz et al. (2007)).

- Difference as a function of instrumental and geophysical parameters.
- Distribution function of the differences, shape, median, mean.
- Geographical patterns: do the patterns look the same?

### 7.2.3 *Use of Models*

Models are used in satellite data validation in three ways:

1. model data (e.g. vertical trace gas distributions) are used to invert satellite measurements in order to obtain tropospheric data (e.g. tropospheric columns),
2. satellite data are used to validate models, and
3. model data are used to validate satellite measurements.

Satellite observations of tropospheric constituents have been used widely to validate models (Velders et al. 2001; Blond et al. 2007; Lauer et al. 2002; de Laat et al. 2007) or to improve the spatial and temporal representation of model emissions (Martin et al. 2003; Müller and Stavrakou 2005; Konovalov et al. 2008). In these studies, the satellite observations are considered providing a “truth” within the bounds of the observation errors, thus serving as reference for the models. This implicitly assumes that the measurements are well characterized and more specifically that their uncertainties are well known. However, as demonstrated for instance by van Noije et al. (2006), differences between individual satellite retrievals of tropospheric composition can be larger than expected from available uncertainty estimates indicating an often incomplete understanding of error sources or error correlations.

The reverse approach, using model information to identify inconsistencies in satellite data, has received comparatively little attention so far. Again a realistic characterization of uncertainties is required but, in this case, of uncertainties in the model data. Satellite measurements have frequently been compared with model output to obtain a basic understanding of the quality of the observations (Buchwitz et al. 2006; de Laat et al. 2007; Yudin et al. 2004) but more quantitative evaluations would be desirable. A valuable approach would be to run a model in parallel with a satellite mission and continuously monitor the differences between model fields and observations. This would help identifying a number of possible algorithm or instrument problems such as:

- scanning/viewing or solar zenith angle dependencies,
- data breaks due to changes in satellite operation procedures or instrumental problems,
- slow degradations in data quality and slow instrumental drifts, and
- seasonal biases.

A data assimilation system in which the satellite observations are incorporated into a model framework can be applied in a similar way. Here the statistics of the observation minus forecast (OMF) errors would have to be monitored (Yudin et al.

2004; Eskes et al. 2003). Of particular use would be a system assimilating multiple independent sources as this would allow identifying inconsistencies between different satellite sensors and not only between observations and model.

Finally, models have been demonstrated to be of great use in validation studies by enhancing the comparability between satellite and *in situ* observations. Ordoñez et al. (2006) and Lamsal et al. (2008), for instance, used model profiles to relate *in situ* surface NO<sub>2</sub> observations to vertical tropospheric columns from satellites. Models, in particular in connection with data assimilation, can also serve to establish a link between different satellite observations taken at different times or different locations. Boersma et al. (2008), for instance, employed the GEOS-CHEM model to estimate the photochemical reduction in tropospheric NO<sub>2</sub> columns between the overpass times of SCIAMACHY (10:00 local time) and OMI (13:30). Similarly, Shindell et al. (2005) showed that a three-dimensional global composition model can be used to account for differences in retrieval sensitivity between two different CO sensors and to account for the spatial and temporal separation of the measurements.

In summary, the potential of models for satellite validation and verification and for data quality monitoring has not yet been fully explored. Assimilation of multiple sources of tropospheric constituent observations appears as a promising pathway for the future as it will greatly augment the comparison possibilities between different satellite sensors and potentially even between sensors measuring different species since they are often closely coupled through chemistry or common sources and sinks.

#### 7.2.4 Data Variability

Part of a proper quality assessment is also the description of the variability of a satellite product in space and time, assessing which part is determined by calibration and retrieval uncertainties, and which part is 'real'. The natural variability of a compound is often quite well known from *in situ* and other remotely sensed observations. Even though *in situ* observations do not provide direct information on volume integrated quantities, they can provide important constraints on the expected variability of a tropospheric column or layer. In addition to the simple consideration of variability at a given location, a comprehensive characterisation of the spatio-temporal behaviour of the product is necessary. This includes a description of the seasonal cycle at different locations and a description of meridional gradients and contrasts between polluted (continental) and remote (oceanic) locations.

A larger than expected variability of satellite data or unexpected seasonal or spatial behaviour may be due to various factors:

- limited precision of the satellite measurement,
- an incomplete separation of the stratospheric signal (Section 7.4.2),

- instrumental and calibration problems not included in the uncertainty estimation,
- wrong assumptions or wrong evaluation of surface albedo or terrain elevation,
- wrong assumptions on the presence or effect of clouds, snow, or ice, and
- wrong use of ancillary data in the retrieval.

A comparison between different OMI NO<sub>2</sub> retrievals, for instance, revealed significant differences in the amplitude of the seasonal cycle pointing towards a significant dependence of the seasonal variation on *a priori* assumptions and the specific retrieval algorithm (Richter et al. 2007).

Some products have been found to exhibit unrealistic contrasts between land- and sea-surfaces or, in the case of near-infrared instruments, to show differences over hot and cold surfaces. At high latitudes, the high solar zenith angles and varying snow and ice covers pose additional problems for the retrieval. A close analysis of the geographic variability will thus help identify some of the problems that introduce unrealistic spatial gradients not seen in ground-based measurements.

Since trace-gas concentrations are usually more variable in the planetary boundary layer than in the free troposphere, the sensitivity of the satellite measurement to the near-surface levels needs to be considered when comparing with other observations. Differences in CO levels between SCIAMACHY and MOPITT, for instance, can partly be attributed to the larger sensitivity of the SCIAMACHY measurement to boundary layer CO (Buchwitz et al. 2007). Such differences can also be expected to affect the amplitude of seasonal cycles and contrasts between polluted and unpolluted regions.

Zhou et al. (2009) demonstrated that using a high-resolution topography data set in satellite retrievals of tropospheric NO<sub>2</sub>, instead of the global low-resolution one which is usually used, has a significant effect on the accuracy of the data over the Alpine region.

As pointed out in the previous section, data assimilation offers great opportunities for analysing the consistency of a satellite product with other observations, particularly for the consistency in observed seasonal and spatial variations. This was demonstrated for instance by Bergamaschi et al. (2007) who compared the temporal and spatial variation in SCIAMACHY CH<sub>4</sub> observations with inverse model simulations that had been optimized versus high accuracy CH<sub>4</sub> surface measurements from the NOAA ESRL network.

### 7.3 Quality Assurance

Quality assurance is a prerequisite of all remote sensing products. Apart from a check on operational quality assurance, the derived impact of algorithm improvements, trends of parameters or degradation processes on the product have to be

taken in account to provide a product that can provide insights over a long period of time.

### 7.3.1 *Validation and Mission Planning*

The satellite mission planning, set-up by the space agencies involved, usually includes several phases which are important to ensure the data quality.

Before launch the main activities to ensure the data quality are the on-ground calibration and the development and testing of the calibration and retrieval software.

The first phase after launch is called the *commissioning phase*, where special measurements are performed to verify the proper performance of all instrument parts.

In the *main validation phase* the satellite instrument is operated optimally for validation measurements. This can be done by measuring over important validation sites or making measurements during campaign periods. Usually several validation campaigns are planned and supported by the agencies for one mission.

Some of the missions also have a *long-term validation phase*. In this phase a few campaigns are planned and routine measurements are collected. This phase is necessary to monitor the data quality over the whole mission duration.

After launch, the agencies perform a day-to-day monitoring of the satellite instrument to detect sudden changes in data quality (Section 7.3.6)

The committee on Earth observation satellites (CEOS) plays an important role in fostering and coordinating interactions between mission scientists and data users. This includes recommendations on network validation sites, development of comprehensive validation methodologies involving ground-based and space-borne assets, and specification of comprehensive and consistent multi-mission validation datasets.

### 7.3.2 *Calibration*

Calibration of instruments, whilst not being the main subject of this chapter is inherently related to validation through its impact on the quality of higher level data products.

For all remote sensing instruments three issues have to be calibrated.

#### **a Viewing Geometry**

The instrument viewing geometry and spatial location of the observed ground scene can be calibrated with fixed Earth targets or high contrast scenes and with the sun, moon or stars.

## **b Wavelength**

The wavelength registration of the instrument detectors can be calibrated by special lamps with spectral lines at fixed wavelengths, or by the well-known Fraunhofer lines in the solar spectrum.

## **c Absolute Radiance**

The radiometric calibration is, for a large part, performed when the instrument is still on the ground. The behaviour of the detectors is studied in detail and as a function of the angle of the incident light, the detector temperature, etc. In flight, changes in the calibration as a function of orbital position are examined, and degradation is monitored (Section 7.3.5).

### **7.3.3 Lower-Level Data Products**

The accuracy of lower level satellite products such as radiance, irradiance, polarisation, and reflectance directly or indirectly influences the accuracy of the higher level products, and the estimated abundances of tropospheric species. Comparison with correlative data and model output is necessary to quantify instrumental spectral features and reflectance offset. On the other hand, long-term studies of higher level data can point to unresolved problems in lower level data.

Lower-level data accuracy is essential to get good geophysical data products. However, it is often necessary to do a first geophysical data validation to have a good idea of lower-level data quality. Trace gas column retrievals are very sensitive to spectral calibration errors. Relative spectral fitting algorithms, like DOAS, can show spectral calibration errors such as shifts and squeezes of the spectrum or bad pixels. Algorithms including those for ozone profile retrieval, AAI retrieval, cloud retrieval, and aerosol optical thickness retrieval, using the absolute reflectance are sensitive to errors in radiometry.

The most important methods of ensuring the quality of the lower-level data products are listed below.

- Geolocation validation: using coastlines, islands, etc.;
- Radiance validation: using radiative transfer modelling (RTM) for the reflectance of selected scenes, such as cloud free deserts, snow/ice, ocean, or bright homogeneous clouds; combine reflectance with reference solar reference spectrum to obtain the radiance (Hagolle et al. 1999; Jaross and Warner 2008);
- Irradiance validation: using solar reference spectrum from literature;
- Reflectance validation: using RTM of selected scenes; comparison with other collocated satellite data (Tilstra et al. 2005); and;
- Polarization validation: using physically acceptable values; using RTM for selected scenes; using the sun as an unpolarised source; comparison with other

collocated satellite data (Tilstra and Stammes 2007; Schutgens and Stammes 2003; Schutgens et al. 2004).

### **7.3.4 Retrieval Algorithm Optimisation**

Demonstration of the validity of a retrieval algorithm is often done for a few specific situations. After implementation of a prototype algorithm in an operational environment and processing of large data sets, the resulting products are carefully verified to find internal inconsistencies and erroneous behaviour. Satellite retrieval algorithms use auxiliary data, retrieval assumptions, and simplifications. These can be valid for certain situations and less valid for others. Specific studies of the validity of the retrieval assumptions for well-chosen datasets directly contribute to the improvement of the algorithm.

Simplifications or misinterpretations of auxiliary data used in the retrieval can result in systematic errors in the retrieved quantities that may depend on geophysical, instrumental or algorithmic parameters. It is important to investigate the influence of these parameter-dependent systematic errors on the intended scientific use. For example, global and regional chemical family budgets might be altered by fictitious spatial structures and temporal signals generated by the retrieval algorithms and superimposed on the actual geophysical signals. Therefore, these systematic errors, dependent on retrieval parameters, should be tracked down systematically and characterised in detail.

As a first stage, prior to performing full geophysical validation of a mature data product, validation has often played and still plays a diagnostic role in the improvement of retrieval algorithms. Careful investigation of comparison time series and the use of assimilation tools have been powerful in revealing internal inconsistencies in satellite data, such as gaps, shifts, systematic biases between data acquired at two different viewing angles, drifts, cycles, etc.

Intercomparisons of satellite data retrieved with independent algorithms have suggested possibilities for improvement.

### **7.3.5 Instrument Degradation**

Instruments in space suffer from ageing caused by a variety of processes including contamination of optical surfaces and the impact of cosmic particles. The effect on the quality of the retrieved satellite data products needs to be carefully monitored. This is especially important with respect to the use of the data products to identify changes or trends in the data product. One important effect is degradation of the optical throughput, especially in the UV. This is caused by UV absorbing species depositing on the optics and reducing the signal-to-noise ratio, impacting on the detection limits and information content of the satellite data products. Cosmic particles hit the detectors periodically, causing an increase in dark current and,

for certain types of detector, introduce a so-called random telegraph signal (RTS). The first of these effects can, in principle, be corrected if there are enough dark current measurements, the second introduces an extra noise term (Dobber et al. 2008). Decreasing signal, increasing dark current, and increasing noise all influence the uncertainty of the satellite products. Long-term validation is necessary to assess the impact of instrument degradation on the data quality.

### **7.3.6 Overall Quality Monitoring**

During calibration, verification and validation studies it becomes clear which parameters can point to instrument, processor, or auxiliary data problems affecting the quality of the resulting satellite products. These parameters are monitored on a day-to-day basis.

Examples of instrumental problems which can have an impact on the data quality are out-of-bounds detector temperatures, partial field of view blocking, contamination, or degradation. Such problems can occur suddenly or gradually and the impact on the data quality cannot always be predicted. A parameter like detector temperature can easily be monitored as it is part of the house-keeping data, but it is less straightforward to detect other instrumental problems.

Sudden processor problems can occur in various situations, such as a new instrument operation mode, an orbit number passing a certain threshold value, or a new processor operating system.

Auxiliary data problems can occur when, for instance, wrong files are used after a change in the processor environment.

Many problems are identified only by chance, because somebody detects unexpected behaviour in the data. In order to detect most problems early it is important that the data are analysed on a daily basis during the complete mission, looking for sudden changes and trends in the estimated retrieval errors and in the quality flags in the product, for different orbital phases, viewing geometries, instrumental modes, etc. It is also possible to detect problems by looking for sudden or gradual changes in the validation results. For this, it is necessary to have many routine correlative measurements of known accuracy taken during the whole mission and well spread over the globe.

Monitoring the data values, retrieval errors and flags, and even a first-order intercomparison with correlative measurements can be automated, but it might be difficult to describe what kind of anomalies should trigger further study. One way of doing it is to determine for each monitoring parameter the mean, median, standard deviation, minimum and maximum values from a well-behaved subset for different orbital phases, viewing geometries, instrumental modes, etc., and define thresholds based on these statistical values. When a parameter gets out-of-bounds it can trigger further manual analysis.

Quality Assurance (QA) software tools, operated by space agencies, undertake part of this quality monitoring. However, these tools do not usually make routine

comparisons with correlative data and lack the more sophisticated algorithms to detect anomalies. They assist the instrument experts to detect anomalies by visual inspection of time series and world maps.

Even in the future when the QA tools become more sophisticated, it will never be possible to detect all problems with such tools, and expert scientific analysis will always remain necessary for the detection of problems with more subtle effects on the data.

## 7.4 Validation Characteristics of Tropospheric Products

In this section, we detail the differences in characteristics of the various tropospheric species, as listed in Table 7.1, which have a direct impact on the validation strategy.

Validation of tropospheric satellite products helps to detect uncertainties related to instrument characteristics and observational technique in combination with retrieval assumptions. Therefore it is important to plan the validation measurements to minimize the spread due to the real variability of the species. Variations that are “real” are principally determined by controlling atmospheric processes such as chemistry, mixing, and long-range transport or can be attributed to an external factor such as the emission profile of a pollutant.

There exists no single best validation strategy applicable to all satellite-borne products related to tropospheric composition (Section 7.6). The relevant issues depend on the actual trace gas and the relevant processes contributing to the spatial distribution and temporal variation of that trace gas. An important assumption in retrievals typically concerns the vertical distribution in the troposphere. Relevant processes that affect the vertical distribution of trace gases are discussed in Section 7.4.1.

The geographical and temporal range of the validation measurements that are needed may differ between different data products. For example, for tropospheric trace gas products a complete validation measurement programme differentiates between cases that are dominated by boundary layer, free troposphere and stratosphere, respectively. The importance of considering stratospheric variations for tropospheric products is explained in Section 7.4.2. The validation measurements should also comprise a set of regions with different concentration level and that are located in different latitude bands and during different months of the year, in order to capture a sufficient variety of relevant chemical regimes and relevant cycles of variations on, say, seasonal and annual scales.

In an observational data record, there are many possible causes for biases and variations. These may partly be caused by instrument limitations such as the signal-to-noise ratio and calibration issues. To a certain extent, biases and variations are also associated with the physical limitations of the applied observational technique. In general, impacts can be expected from the observation geometry, the actual temperature and humidity profile, cloudiness, land surface characteristics, etc. Retrieval

algorithms minimize these impacts where parameterizations and/or corrections are applied. A major impact on trace gas retrievals is expected from the assumptions about clouds, aerosols and the Bidirectional Surface Distribution Function. These are discussed briefly in Section 7.4.3.

### ***7.4.1 Tropospheric Processes Impacting on Trace Gas Distributions***

An important time scale with respect to the horizontal distribution of trace gases is the time scale for a plume (e.g. an emission pulse, or a stratospheric intrusion) to dissolve in the background. The time period can be very short, in the case where the plume quickly encounters a strong mixing event or in the case of fast chemical degradation, but typically is of a couple of days up to about 2 weeks.

Most variations on longer-lived pollutants occur in the boundary layer and are related to emission profiles such as rush hours, imperfect mixing and, in the case of ozone, the possibility of rapid ozone formation by fast chemistry under stagnant and warm polluted conditions.

Imperfect knowledge of the trace gas vertical profile in the troposphere is an important contribution to the overall uncertainty for tropospheric trace gas retrievals (Boersma et al. 2004), and therefore also for the validation of these retrievals. For most satellite measurement techniques, the sensitivity of the measurement is a function of altitude in the troposphere. This is true, for example, for measurements of the solar radiation backscattered in the UV-Vis range (observation of  $\text{NO}_2$ ,  $\text{SO}_2$ ,  $\text{HCHO}$ ,  $\text{O}_3$ ) as well as for measurements of the thermal emission (observation of  $\text{CO}$ ,  $\text{CH}_4$ ,  $\text{O}_3$ ). The  $\text{NO}_2$  vertical profile in the troposphere is highly variable in time and location and typically determined by a set of interacting processes.  $\text{NO}_x$  emissions and dry deposition (Ganzeveld and Lelieveld 1995) occur near the surface, while photochemistry and turbulent mixing are important within the boundary layer. In the free troposphere, long-range transport, wet removal, convection and lightning may significantly influence the vertical distribution. Some  $\text{NO}_x$  is injected at higher altitudes by pyro-convection related to biomass burning, and by aircraft emissions. Finally, the concentration of  $\text{NO}_2$  in the atmosphere is in a photochemical steady state with the concentration of  $\text{NO}$ ,  $\text{N}_2\text{O}_5$ ,  $\text{O}_3$  and  $\text{ClO}$ , the steady state depending on the ambient temperature, through the Arrhenius equation, and UV light intensity, the actinic flux, having a strong dependence on solar zenith angle and cloudiness. Thus the  $\text{NO}_2$  vertical profile will typically undergo rapid changes during a day, some of the changes being recurrent, for example, the diurnal cycle, others being much less predictable such as the effects linked to the presence of clouds and of turbulent transport. Because of the large number of possible processes involved, the validation of  $\text{NO}_2$  is challenging. Satellite-to-satellite intercomparison offers some advantages because of the collocation and similarity in spatial representativity. Validation with ground-based remote sensing can offer

the advantage of similarities in vertical sensitivity and, for tropospheric data retrieved using residual methods (the tropospheric column is obtained by subtracting from the satellite total column measurement an estimate of the stratospheric column), the possibility of discriminating between the stratospheric and tropospheric contributions to the total column measured by the satellite. Validation with *in situ* observations of  $\text{NO}_2$  is very complicated, especially close to emission sources.

Fig. 7.8 shows a satellite-to-satellite comparison of SCIAMACHY and OMI  $\text{NO}_2$  tropospheric columns. The purpose of the comparison by Boersma et al. (2008) was to examine the consistency between the two instruments under tropospheric background conditions and the effect of different observation times. The example illustrates the difficulty to distinguish deviations due to “real” atmospheric processes from deviations generated artificially by differences in instrument and/or retrieval characteristics.

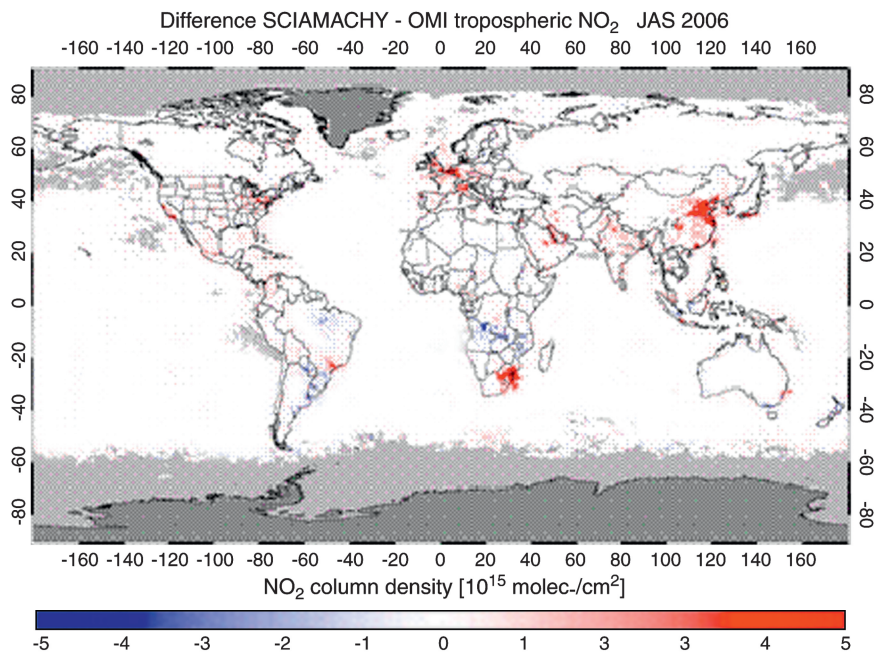


**Fig. 7.8** Difference between SCIAMACHY and OMI tropospheric  $\text{NO}_2$  columns for the period July-August-September 2006. From a careful analysis of the consistency between SCIAMACHY and OMI tropospheric  $\text{NO}_2$  observations in different regions of the world it was concluded that part of the difference could be attributed to the diurnal cycle in emissions and photochemistry. Morning SCIAMACHY  $\text{NO}_2$  is higher than afternoon OMI  $\text{NO}_2$  over fossil fuel source regions because of photochemical loss in combination with a broad daytime emission profile, and lower than OMI over tropical biomass burning source regions because of a sharp mid-day peak in  $\text{NO}_x$  emissions as confirmed by fire counts. (from Boersma et al. (2008)).

Although different in detail, similar types of challenges exist for other species. HCHO, CHOCHO, BrO, and SO<sub>2</sub> are short-lived (~hours) and undergo rapid changes during the day in a similar way to NO<sub>2</sub>. Water vapour changes in the atmosphere are also rapid, though related to fast processes in the hydrological cycle, including evaporation from the surface, cloud/rain formation, and cloud/rain evaporation. Transport and imperfect mixing in the boundary layer and free troposphere further contribute to water vapour variability on the kilometre scale. Validation of short-lived products is necessarily complex as it should cover a large range of time scales both unpolluted and polluted locations with different chemical regimes, meteorological conditions and emission profiles.

CO, tropospheric O<sub>3</sub> and CH<sub>4</sub> are longer-lived tropospheric gases with chemical lifetimes ranging from days to years. Free-tropospheric variability is mainly related to convection and synoptic scale variability. These are most important for long-range, intercontinental, transport. Stratosphere-troposphere exchange is an important contributor to variations in tropospheric O<sub>3</sub>. Stratospheric O<sub>3</sub> intrusions may penetrate deep into the free troposphere before mixing (Roelofs et al. 2003).

It is important for validation that the methods capture the most relevant processes that may contribute to the variation in the product. When different time scales are involved, complex and non-linear relationships may exist between observed variations, instrument and observational technique related variations, and physical/chemical/meteorological controlling processes and factors. Fig. 7.9 shows a comparison of SCIAMACHY CO columns with MOPITT CO columns (de Laat et al. 2010). The explanations of the differences are given in the caption and illustrate the complexities that arise in the comparison of two independent data sets.

### ***7.4.2 Validation Needs for Trace Gases with Stratospheric Contributions***

While some species are present primarily in the troposphere, other species may also have a high concentration in the stratosphere, in between the tropospheric target and the satellite. The retrieval of tropospheric columns of O<sub>3</sub>, NO<sub>2</sub> and BrO often involves the subtraction of an estimated stratospheric part (Section 2.4). The uncertainty of tropospheric data products will probably be larger above regions where the stratospheric variability is large. Validation can contribute to a better understanding of the error sources of the retrieval methods, especially when it includes verification of the assumed stratospheric contributions and the assumed profile shapes with independent measurements.

#### **a What Causes Stratospheric Variability?**

In the stratosphere, and in particular in the lower stratosphere, many trace gases including O<sub>3</sub>, CH<sub>4</sub>, and the reactive chlorine and nitrogen oxide families, Cl<sub>y</sub> and

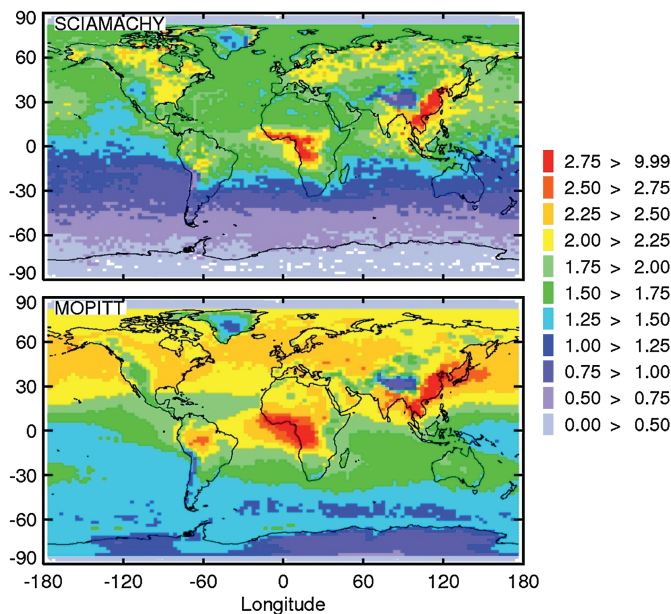


**Fig. 7.9** Comparison of CO columns from SCIAMACHY (*top*) and MOPITT (*bottom*). Averages of the period 2004–2005 are shown in  $10^{18}$  molecules/cm<sup>2</sup> on a  $3^\circ \times 2^\circ$  resolution. The grey areas indicate regions without observations. Common features are the hemispheric gradient and the emission patterns over tropical biomass burning areas and in eastern Asia. De Laat et al. (2010) showed that there is a bias between the CO columns from both instruments and explain the differences as being related to instrumental precision (SCIAMACHY is somewhat noisier), weighting assumptions (SCIAMACHY is weighted with the noise error), error-covariance and *a priori* assumptions in the retrievals and some other effects, such as the presence of aerosols, differences in spectroscopy of interfering gases such as CH<sub>4</sub> and H<sub>2</sub>O and the ice-layer correction to SCIAMACHY. (from de Laat et al. (2010)).

NO<sub>y</sub>, have chemical lifetimes considerably longer than the time scales of planetary and synoptic scale wave activity. Their variability is principally dominated by dynamic processes and, consequently, is typically largest at middle and high latitudes. There are exceptions, such as O<sub>3</sub> in polar springtime when its chemical lifetime becomes shorter due to rapid destruction in catalytic reactions with halogen radicals activated on the surfaces of polar stratospheric clouds and aerosols. Here, the variability is caused by a mixture of chemical and dynamical processes. Individual species of a reactive gas family may have much shorter lifetimes and exhibit a pronounced diurnal cycle. A good example is NO<sub>2</sub>, which is rapidly photolysed to NO and oxidized by O<sub>3</sub> to NO<sub>3</sub> but is continuously reformed from its products, resulting in a pronounced diurnal cycle of NO<sub>2</sub>, whereas the sum NO<sub>x</sub> (NO + NO<sub>2</sub> + NO<sub>3</sub> + 2 N<sub>2</sub>O<sub>5</sub>) is fairly constant throughout the day. Such rapid diurnal variations in the partitioning within a compound family therefore need to be accounted for, as well as the variability induced by dynamic processes.

In the retrieval of  $\text{NO}_2$ ,  $\text{CH}_4$  and  $\text{CO}_2$ , assumptions are made on the vertical distribution of these species (Section 2.3.3). The uncertainty of the tropospheric products might therefore be larger over regions with a deviating or variable vertical distribution.

## **b What Determines the Vertical Distribution of these Species?**

The distribution of trace gases in the atmosphere is generally determined by the distribution of sources and sinks and by transport processes. Vertical exchange is influenced by the temperature profile that determines the (dry) static stability of the profile, as well as by turbulent and convective processes and mixing, and by quasi-horizontally moving air masses crossing in different directions at different altitudes.

Vertical exchange is largely suppressed in regions of high stability, which are therefore regions of enhanced vertical trace gas gradients. The temperature inversion at the top of the boundary layer, for example, separates the (potentially) polluted air in the boundary layer from the cleaner air in the free troposphere. Exchanges between boundary-layer and free troposphere are dominated by orographic effects, the uplift of air masses in warm conveyor belts associated with frontal systems, entrainment and turbulent mixing, cloud processes, and the daily decoupling of the residual layer from the surface as soon as a new inversion appears near the surface at the end of the day.

Another region of high stability is the tropopause inversion which separates tropospheric and stratospheric air masses. In the extratropics, cross-tropopause exchange is dominated by synoptic scale processes and occurs mostly in tropopause folds and cut-off lows generated by baroclinic disturbances in the mean jet stream (Holton et al. 1995). The disturbances are often associated with mesoscale convective complexes and thunderstorms. At tropical latitudes, convectively driven air masses may enter the tropical tropopause layer and subsequently reach the stratosphere by much slower diabatic ascent. The total mass of air entering the stratosphere in the tropics is controlled by the “extra-tropical pump” which drives the Brewer-Dobson circulation (Holton et al. 1995). During exceptionally strong volcanic eruptions aerosols and  $\text{SO}_2$  can also reach the stratosphere directly. At higher latitudes, downward motions are dominant and the descending stratospheric air mixes within the troposphere.

The amount of  $\text{O}_3$  in the troposphere is an order of magnitude smaller than in the stratosphere. This makes it difficult to retrieve from satellites (Sections 2.4 and 2.5.5), especially in regions where the stratospheric variability is large. Validation analysis of tropospheric ozone should include the distinction between the regions with different stratospheric variability.

The column amount of tropospheric  $\text{NO}_2$  above polluted areas is comparable to or larger than the stratospheric part, while above clean areas it is much smaller. Validation analysis should include a progressive distinction from polluted to clean areas.

Also validation analysis for methane should account for stratospheric column variations, which are of the same order as the tropospheric variations caused by emissions and free tropospheric gradients. Total column BrO is typically confined to the stratosphere, with significant tropospheric contributions confined to very specific conditions such as springtime at the edge of first-year sea ice.

### 7.4.3 Validation Needs Related to Cloud, Albedo and Aerosol Effects

Retrievals of tropospheric gases can be severely affected by the presence of clouds. Clouds shield tropospheric gases from observation, but may also enhance the sensitivity to trace gases above the cloud in the case of measurements with reflected sunlight. Not only clouds, but also aerosols and surface albedo influence the light path in the atmosphere and thereby affect tropospheric trace gas measurements. The actual light path can be measured by using oxygen absorption (using the O<sub>2</sub> A-band and O<sub>2</sub>–O<sub>2</sub> lines for example), since oxygen is well mixed. In addition, Raman scattering can be used.

Some retrieval algorithms of tropospheric species, for example, NO<sub>2</sub>, only select cloud-free scenes and do not correct for clouds. Other retrieval algorithms correct for the presence of clouds. In the latter case, most algorithms use a simple Lambertian cloud model for the correction in which a surface with high albedo at some pressure level is assumed for the cloud (Koelemeijer et al. 2001; Van Roozendaal et al. 2006; Veeffkind and de Haan 2001; Boersma et al. 2004). The two parameters in the Lambertian model are the effective cloud fraction and effective cloud pressure (Stammes et al. 2008 and Chapter 5). A scattering cloud model has more parameters: geometric cloud fraction, cloud optical thickness, cloud top and bottom pressures, and the possible presence of multiple cloud layers. Such a model needs more auxiliary data or *a priori* assumptions (van Diedenhoven et al. 2007).

The validation requirements for clouds depend on the trace gas retrieval algorithm. For the algorithms that only need cloud-free scenes, a high quality cloud mask is needed. This is usually derived from a radiance threshold, but can also be derived from high resolution imagery collocated with the trace gas data. Alternatively, the effective cloud fraction can be used because it gives the radiometric weight of clouds in the scene, which is needed in air mass factor calculations. The radiometric weight,  $w$ , is defined as the fraction of radiation coming from clouds in the pixel. In the case of the Lambertian cloud model (Stammes et al. 2008):

$$w = cR_c/R_{tot} = c_{eff}A_c/R_{tot} \quad (7.2)$$

Here  $c$  is the geometric cloud fraction,  $c_{eff}$  is the effective cloud fraction assuming a cloud with albedo  $A_c$ ,  $R_c$  is the reflectance of the cloud and  $R_{tot}$  is the

measured reflectance of the satellite pixel. In general, it is necessary to validate the product  $c_{eff} A_c$ .

Cloud properties used in cloud correction algorithms can be validated by comparison with dedicated cloud instruments, such as multi-spectral imagers. In these comparisons, the interpretation of the oxygen absorption cloud properties is important. It has been found that the oxygen cloud pressure, retrieved using a Lambertian cloud retrieval model, does not represent the cloud top pressure, but rather the pressure at a level inside the cloud or between the cloud layers (Sneep et al. 2008; Wang et al. 2008). This is due to the multiple scattering of solar photons inside the cloud. On the other hand, the cloud pressure given by satellite imagers in the thermal IR is the top of the cloud, because IR radiation is emitted from the top of the cloud. Since clouds are strongly absorbing in the IR, IR radiation hardly penetrates through the clouds.

For cloud validation, comparison with other satellite sensors is essential because of the variability of clouds. Most useful are cloud imagers, which have visible, shortwave IR and thermal IR channels for determination of the geometric cloud fraction, optical thickness and cloud top pressure. Cloud radar and lidars from space or ground are important to determine “true values” of cloud top pressure, and cloud mid-level and cloud bottom pressure. Table 7.2 gives an overview.

An important characteristic of clouds is their high variability in time and global variation. Single clouds typically live less than an hour. Statistically, clouds have diurnal cycles depending on the region. Furthermore, cloud types vary over the globe, and detection of clouds depends on the surface albedo. Therefore, it is insufficient to validate at a few specific sites where ground-based instruments are located. The opportunity to validate cloud retrievals with the cloud radar/lidar

**Table 7.2** Main cloud parameters for tropospheric trace gas retrievals, their needed accuracy, and sources of validation

Cloud parameter	Symbol	Needed accuracy	Comparison/validation source	Note
Effective cloud fraction	$c_{eff}$	0.05	Cloud imager	Compute $c_{eff}$ from $c$ and $\tau$ of imagery data
Effective cloud pressure	$p_c$	100 hPa	Cloud radar	O <sub>2</sub> absorption and Raman scattering give mid-cloud level
Cloud mask	–	5%	Cloud imager	Cloud-free scene selection
Geometric cloud fraction	$c$	0.1	Cloud imager	Scattering cloud model
Cloud optical thickness	$\tau$	10 %	Cloud imager	Scattering cloud model
Cloud top pressure	$p_{top}$	100 hPa	Cloud imager Cloud radar/lidar	Scattering cloud model
Cloud bottom pressure	$p_{bot}$	100 hPa	Cloud radar/lidar	Scattering cloud model

CloudSat/CALIPSO in the A-train is unique for satellite trace gas retrievals (Sneep et al. 2008).

Before validation can be performed, a statistically significant verification of the cloud product is needed. One should verify the quality of cloud retrievals by analysing global cloud retrievals and checking for consistency and absence of jumps depending on the viewing geometry, solar zenith angle, latitude, etc. This verification process can be done easily by using the CAMA tool (Sneep et al. 2006), which is an IDL programme correlating all parameters of a data product with one another. The CAMA tool has been used extensively in the validation of OMI data (Sneep et al. 2008; Stammes et al. 2008; Kroon et al. 2008).

Surface albedo is an important auxiliary parameter needed for trace gas, aerosol and cloud retrievals from satellite. A high surface albedo increases the sensitivity of satellite measurements to tropospheric trace gases, but decreases the sensitivity to (scattering) aerosols. Often a surface albedo climatology is used, for example, the GOME climatology of Koelemeijer et al. (2003) or the OMI climatology of Kleipool et al. (2008). If the assumed surface albedo is not correct, say, due to insufficient spatial resolution, the trace gas amount for the clear sky part of the pixel will be incorrect. However, since the detected cloud fraction will also be incorrect for an incorrect surface albedo, there will be some compensation taking place for the total pixel (cloud-free plus cloudy parts), since cloud fraction will be adjusted to match the reflectance at top of atmosphere. For this compensation it is important that the trace gas and cloud retrievals use the same surface albedo data base. In the validation of trace gases, the cloud information should be taken into account.

The impact of aerosols (Chapter 6) is not explicitly included in trace gas retrievals, but it could be a significant error. In most algorithms aerosols are included implicitly as a type of clouds, which may work for scattering aerosols, but not for absorbing aerosols. This is still a largely unexplored topic, which is relevant for highly polluted regions.

#### ***7.4.4 Validation Needs for Aerosols***

Chapter 6 describes the details of aerosol retrievals from satellites. Passive measurements yield column integrated aerosol parameters such as AOD, the column integrated aerosol extinction. Active instruments such as a lidar, for example CALIOP on CALIPSO, part of the A-train, provide information on the vertical structure. Instruments with multiple viewing angles (MISR, POLDER, ATSR) can be used to determine the 3-D structure of plumes (Kahn et al. 2007).

Independent data of aerosol physical, chemical, and optical properties are needed to validate the retrieval results. Since the retrieval uses several assumptions on surface and atmosphere parameters, information should also be available on the boundary layer structure and meteorological parameters. These data and additional information can be obtained from dedicated campaigns and networks.

The AERONET network (Holben et al. 1998) was established to obtain information on the aerosol optical properties for satellite validation. Instruments used are CIMEL sun photometers which provide both direct sun measurements and almucantar scans from which information can be derived on the column-integrated aerosol physical and optical properties such as AOD, effective radius and complex refractive index. Lidars provide extinction and backscatter profiles (raman lidars used in the EU-funded EARLINET network) which are used to evaluate CALIOP measurements. Lidar measurements can be integrated to provide the AOD. Lidar measurements provide a very sensitive way to detect cloud reflections, even for sub-visible clouds which can have an adverse effect on aerosol retrieval. A recent comparison of lidar and AERONET data shows that AERONET is very effectively cloud screened (Schaap et al. 2009).

The effect of the surface correction used in the retrieval could in principle be evaluated by comparison with these instruments if the path radiance could be accurately obtained. However, this is usually not the case and the uncertainty in satellite retrieved AOD is larger than that obtained from sun photometers (typically on the order of 0.03 over ocean or 0.05 over land (Robles-Gonzalez et al. 2006), whereas the accuracy of CIMEL sun photometers used in AERONET is between 0.01 and 0.015 (Eck et al. 1999)).

In order to quantify the uncertainties in the aerosol products for clouded scenes it is necessary that the clouded scenes are validated. The cloud mask used in the aerosol retrieval should also be validated and it should be verified that it does not remove aerosol, as might be the case for large AODs from desert dust storms or smoke.

## 7.5 The Use of Correlative Measurements for Validation

For validation purposes a comprehensive set of correlative data is needed, either acquired during a specially designed short period calibration/validation campaign or used from long term monitoring networks or other special programmes. The correlative data sets ideally comprise collocated ground-based *in situ* and remote sensing of tropospheric and stratospheric profiles and columns, as well as airborne measurements. In this section, the different measurement techniques and their characteristics for validation are discussed. The networks and data centres are summarised in Section 7.5.3 and in Tables 7.3–7.5.

### 7.5.1 *In Situ Measurements*

Several measurement techniques are currently used for the validation of tropospheric satellite products.

Table 7.3 *In situ* ground based networks and their data centres

Programme	Parameters	Data centre	QA/QC	Web address
EEA/EU	Reactive Gases	Airbase	Yes	<a href="http://dataservice.eea.europa.eu/dataservice/metadetails.asp?id=1029">http://dataservice.eea.europa.eu/dataservice/metadetails.asp?id=1029</a>
UN-ECE	Reactive gases and chemistry	EMEP/CCC	Yes	<a href="http://www.milu.no/projects/ccc">http://www.milu.no/projects/ccc</a>
WMO/GAW	GHGs and reactive gases	WDCGG	Yes	<a href="http://gaw.kishou.go.jp/wdceg">http://gaw.kishou.go.jp/wdceg</a>
WMO/GAW	Radiation	WRDC	Yes	<a href="http://wrdc.mgo.rssi.ru">http://wrdc.mgo.rssi.ru</a>
WMO/GAW	Aerosol and AOD	WDCA	Yes	<a href="http://www.gaw-wdca.org">http://www.gaw-wdca.org</a>
WMO/GAW	Precipitation	WCDPC	Yes	<a href="http://www.qasac-america.org">http://www.qasac-america.org</a>
WMO/GAW	Ozone and UV	WOUDC	Yes	<a href="http://www.woudc.org">http://www.woudc.org</a>
NOAA	GHGs and reactive gases & aerosols	GMD Data Archive		<a href="http://www.esrl.noaa.gov/gmd/dv/ftpdata.html">http://www.esrl.noaa.gov/gmd/dv/ftpdata.html</a>
US national	Climate variables	NCDC		<a href="http://www.ncdc.noaa.gov/oa/ncdc.html">http://www.ncdc.noaa.gov/oa/ncdc.html</a>
NASA/US	Aerosol/Radiation	AERONET	Yes	<a href="http://aeronet.gsfc.nasa.gov">http://aeronet.gsfc.nasa.gov</a>
PHOTONS	Aerosol/Radiation	PHOTONS	Yes	<a href="http://loaphotons.univ-lille1.fr">http://loaphotons.univ-lille1.fr</a>
EUSAAR	Harmonized aerosol data	NILU/IBAS	Yes	<a href="http://www.eusaar.net">http://www.eusaar.net</a>
GEOmon	Trop. and strat. gases and aerosols	NILU/EBAS	Yes	<a href="http://www.geomon.eu/data.html">http://www.geomon.eu/data.html</a>

**Table 7.4** Remote sensing, balloon and aircraft networks and data centres

Programme	Parameters	Data centre	QA/QC	Web address
NDACC	Remote sensing	NDACC	Yes	<a href="http://www.ndacc.org">http://www.ndacc.org</a>
WMO/GAW	Ozone profiles	WOUDC	Yes	<a href="http://www.woudc.org">http://www.woudc.org</a>
SHADOZ	Ozone sondes			<a href="http://croc.gsfc.nasa.gov/shadoz">http://croc.gsfc.nasa.gov/shadoz</a>
CARIBIC	aeroplane	CERA		<a href="http://www.caribic-atmospheric.com">http://www.caribic-atmospheric.com</a>
EARLINET	Aerosol lidars			<a href="http://www.earlinet.org">http://www.earlinet.org</a>

### a *In Situ* Measurements for O<sub>3</sub> and CO

Tropospheric O<sub>3</sub> can be inferred from *in situ* O<sub>3</sub> profiles, as measured by ozone sondes (types: Electrochemical Concentration Cell (ECC), Brewer-Mast, Carbon-Iodine) and by aircraft (UV ozone analyser) during take-off and landing. O<sub>3</sub> soundings are performed between 1 and 3 times a week as part of a continuous program or during special validation campaigns. There are a number of operational ground stations that perform this type of measurements on a regular basis. Most of these submit their data to WOUDC (World Ozone and Ultraviolet radiation Data Centre). This UV/ozone network is part of WMO and is operated by the Meteorological Service of Canada. A smaller and more recent NASA funded network is the SHADOZ (Southern Hemisphere ADDitional OZone sondes) network, which focuses on the tropics. The network has been operational since 1998. SHADOZ ozone-sondes operate at different frequencies, all use ECC of various types; twelve active sites participate, and they are also included in the WOUDC network.

*In situ* measurements are also acquired from UV ozone analysers (Thermo-Electron, Model 49-103) on board the passenger airliners that take part in MOZAIC. This program, which was initiated in 1993, focuses on several species including O<sub>3</sub> and CO. Most of the data (90%) are collected at cruise altitudes of 9–12 km. At mid-latitudes this altitude region covers the tropopause, a region critical for climate change and the exchange between stratosphere and troposphere. The remaining data is acquired during ascents and descents at airports visited by the program.

A less extensive but detailed database has been building up since 2004 in the framework of the CARIBIC project. Measurements of O<sub>3</sub> and CO and a number of other species are made during long distance flights with an Airbus A340-600 from Lufthansa. The ozone analyzer operates with two different measuring principles: a fast O<sub>3</sub> analyzer using fluorescence of an organic dye absorbed on silica gel and a standard O<sub>3</sub> analyzer using UV absorption.

*In situ* flask measurements are harmonized in the NOAA/ESRL/GMD CCGG cooperative air sampling network. This is a globally distributed network of sites taking regular discrete samples and which includes the 4 NOAA ESRL/GMD baseline observatories, cooperative fixed sites, and commercial ships (<http://www.esrl.noaa.gov/gmd/ccgg/flask.html>). Air samples are collected on a weekly basis and are analysed in Boulder for CO and a variety of other gases.

Table 7.5 Satellite data centres

Programme	Parameters	Data centre	QA/QC	Web address
NDMC/WMO	Satellite	WDC-RSAT		<a href="http://wdc.dlr.de">http://wdc.dlr.de</a>
US national	Climate variables	NCDC		<a href="http://www.ncdc.noaa.gov/oa/ncdc.html">http://www.ncdc.noaa.gov/oa/ncdc.html</a>
CEOS	satellites	CAL/Val portal		<a href="http://calvalportal.ceos.org">http://calvalportal.ceos.org</a>
ESA airborne campaigns	Satellite related	ESA EO campaign		<a href="http://earth.esa.int/campaigns">http://earth.esa.int/campaigns</a>
ESA	<i>In situ</i> , remote sensing & satellite	EVDC		<a href="http://nadir.nilu.no">http://nadir.nilu.no</a>
NASA	Aura	AVDC		<a href="http://avdc.gsfc.nasa.gov">http://avdc.gsfc.nasa.gov</a>
NASA	Aerosols	MODIS	Yes	<a href="http://modis-atmos.gsfc.nasa.gov">http://modis-atmos.gsfc.nasa.gov</a>
NASA	Aerosols	Giovanni	Yes	<a href="http://disc.sci.gsfc.nasa.gov/giovanni/overview">http://disc.sci.gsfc.nasa.gov/giovanni/overview</a>
ICARE	Aerosols	ICARE	Yes	<a href="http://www.icare.univ-lille1.fr">http://www.icare.univ-lille1.fr</a>
ESA-DUE	Aerosols, trace gases, clouds	TEMIS		<a href="http://www.temis.nl">http://www.temis.nl</a>
ESA-GSE	Aerosols & trace gases products	PROMOTE		<a href="http://www.gse-promote.org">http://www.gse-promote.org</a>
WMO-GAW	Aerosols	WDC-RSAT		<a href="http://wdc.dlr.de">http://wdc.dlr.de</a>

For *in situ* surface measurements of  $O_3$  and  $CO$ , the uncertainty contribution resulting from different measurement techniques used in monitoring networks (Klausen et al. 2003; Zellweger et al. 2009) are considered negligible for satellite validation purposes.

## **b *In Situ* Measurement Techniques for $NO_2$**

For  $NO_2$  the choice of the measurement technique is crucial, since many of the measurement principles used in *in situ* monitoring networks are not specific for the  $NO_2$  detection. Depending on the method and the atmospheric photochemical conditions, interference from non- $NO_2$  compounds may exceed the  $NO_2$  concentration by up to 250%, because not only  $NO_2$  but also some fraction of the rest of  $NO_y$  ( $NO_y = NO + NO_2 +$  peroxy nitrates + alkyl and multifunctional nitrates +  $HNO_3 + \dots$ ) is converted (Steinbacher et al. 2007). For satellite validation, data with low or well defined interference are required.

There are several other specific techniques available to measure  $NO_2$  at atmospheric levels, such as DOAS (Alicke et al. 2002; Platt and Perner 1980), chemiluminescence induced by the reaction with luminol (Kelly et al. 1990), TDLAS (Li et al. 2004), laser induced fluorescence (LIF) (Murphy et al. 2006; Cleary et al. 2002; Day et al. 2003; Matsumoto et al. 2001), or by pulsed cavity ring-down spectroscopy (Kebabian et al. 2005; Osthoff et al. 2006). Recently, more and more *in situ* networks replace non-specific converters with photolytic converters, specific for  $NO_2$ . The two most prevalent techniques currently used for validation are LIF detection of  $NO_2$  and conversion of  $NO_2$  to  $NO$  followed by detection of  $NO$  with chemiluminescence (CL). In LIF, a laser is used to excite  $NO_2$ , which then fluoresces. CL detection of  $NO$  relies on titrating it with  $O_3$  to produce excited  $NO_2$ , which then emits an amount of light proportional to the concentration of  $NO$ . Systems employing either LIF or CL are calibrated with gravimetrically prepared standards.

On airborne platforms such as the DLR Falcon, the NASA C130, the NOAA P-3 and others that use CL,  $NO_2$  is converted to  $NO$  photolytically, which is a specific conversion. On board NOAA's Ron Brown Research vessel,  $NO_2$  has been measured by  $NO_2$  specific pulsed cavity ring-down spectroscopy (Osthoff et al. 2006).

The first reported comparison of tropospheric  $NO_2$  columns from satellite observations with *in situ* aircraft data was between GOME and the Falcon aircraft and took place over Austria in early May 2001 (Heland et al. 2002). Since then there have been numerous opportunities for comparison between the GOME, SCIAMACHY and OMI satellite instruments and a number of different mobile platforms. In some cases, ground-based measurements have been used to deduce independently an *in situ* column for comparison to the satellites (Schaub et al. 2006).

### c Factors Impacting on the Use of *In Situ* Measurements for Satellite NO<sub>2</sub> Data Validation

There are a number of factors concerning both the collection and the subsequent treatment of *in situ* data that must be considered when using observations from mobile or ground-based platforms to generate *in situ* NO<sub>2</sub> columns for comparison with satellite columns. The fundamental problem arises when attempting to compare data taken at a single point (for ground sites) or a point-wise representation of a portion of the column (for airborne platforms) with satellite data, the latter being integrated in both the horizontal and vertical dimensions.

Except for remote locations, the vast majority of the tropospheric NO<sub>2</sub> column is concentrated in the boundary layer, which means that uncertainties and extrapolations of observations within the boundary layer will affect the calculated *in situ* column disproportionately as compared to uncertainties and extrapolations of data in the free troposphere. Aircraft observations require extrapolation from the lowest elevation achieved to ground level while ground-based observations require upward extrapolation. Thus, when using an aircraft platform, sampling within the boundary layer is essential and attempts should be made to sample the column at the lowest possible elevation that safety allows. In addition, in the case of aircraft observations that span several satellite pixels, it is essential to compare only those pixels for which there are *in situ* observations within the boundary layer. Similarly, if ground-based NO<sub>2</sub> observations are to be used, it is essential that they be accompanied by a reliable measurement of the boundary layer depth.

If the widespread existing network of ground-based NO<sub>x</sub> sensors is to be used for satellite comparisons, we must assess and quantify accurately the conversion of other NO<sub>y</sub> species to NO<sub>2</sub> when using catalytic conversion chemiluminescence. In general, these systems see a positive interference in NO<sub>2</sub> and will thus overestimate boundary layer NO<sub>2</sub>, but the magnitude of the interference will vary on a site-to-site basis. The NO<sub>x</sub>/NO<sub>y</sub> ratio is known to decrease with photochemical aging as NO and NO<sub>2</sub> are converted to higher order NO<sub>y</sub> species so, to a first approximation, the interference will be largest at ground sites that are far removed from source regions and which sample well-aged air masses.

#### 7.5.2 Remote Sensing

Remote sensing observations from the ground can bridge the gap between satellite columns and surface *in situ* measurements. Using similar techniques as the satellite instruments, they determine the tropospheric columns with good accuracy and sometimes with similar sensitivity to the vertical distribution of the species.

### **a Multi-Axis Differential Optical Absorption Spectroscopy (MAXDOAS)**

Based on the measurement principles pioneered by Dobson and Harrison (1926), DOAS has been used for about three decades to measure amounts of O<sub>3</sub>, NO<sub>2</sub>, HCHO, BrO, and many other trace gases in the atmosphere (Brewer et al. 1973; Noxon 1975; Platt and Perner 1980; McKenzie and Johnston 1982; Solomon et al. 1987; Pommereau and Goutail 1988a, b). The MAXDOAS technique (Sinreich et al. 2005) to measure aerosol profiles has recently been explored and first results are promising. When using scattered sun light as the light source, a high degree of automation can be obtained and measurements can be taken independently of weather conditions. Originally, DOAS measurements were performed for stratospheric studies and the instrument's telescopes pointed towards the zenith to minimise the impact of tropospheric absorptions. In this viewing geometry, very large sensitivity is obtained for stratospheric absorbers at twilight when the light path in the upper atmosphere is long before the photons are scattered and pass vertically through the lower troposphere before they reach the instrument. In the framework of the international Network for the Detection of Atmospheric Composition Change (NDACC), a contributing network of WMO's Global Atmosphere Watch, over 35 zenith-sky DOAS spectrometers currently perform network operation from the Arctic to the Antarctic. Most of them are located in remote areas characterised by a very clean local troposphere.

Among them, about 50% operate in areas where no significant pollution can be detected at spatial scales of the order of a nadir-viewing satellite pixel. This feature and the enhanced sensitivity to stratospheric absorbers make these spectrometers well suited for validating the satellite column data over clean areas, as well allowing estimates of the stratospheric column to be made by satellite retrieval algorithms based on the residual technique. Most of the NDACC DOAS/UV-visible spectrometers monitor the vertical columns of O<sub>3</sub> and NO<sub>2</sub>. The network allows validation studies for NO<sub>2</sub> in the range from 10<sup>14</sup> molecules/cm<sup>2</sup> during polar winter up to 6.5 × 10<sup>15</sup> molecules/cm<sup>2</sup> in polar summer, and under small solar zenith angles to twilight conditions. A few NDACC spectrometers also measure the column abundance of stratospheric BrO and OCIO.

In 1993, Sanders et al. (1993) added complementary viewing directions to increase the signal-to-noise ratio of stratospheric absorptions and they noticed that off-axis measurements also increase the sensitivity to tropospheric absorbers. Resulting multi-axis or MAXDOAS measurements (Hönninger and Platt 2002; Hönninger et al. 2004b; Wittrock et al. 2004) are based on the idea that very long light paths in the lower troposphere are achieved when pointing the telescope to the horizon while the stratospheric light path is largely independent of the pointing of the telescope. By combining the measurements from different viewing directions, vertical profile information can be retrieved on the lower troposphere in much the same way as for limb measurements from balloon and satellite instruments. The profile information is valuable for atmospheric chemistry applications and satellite validation but it also improves the accuracy of the primary measurement quantity of

MAXDOAS measurements, the tropospheric columns. Fig. 7.10 shows two MAXDOAS instruments in operation.



Fig. 7.10 MAXDOAS instruments at the University of Bremen.

In recent years, a number of studies have been performed using MAXDOAS measurements for the investigation of pollution events (Heckel et al. 2005; Leigh et al. 2006), for studies of halogen oxide chemistry in high latitudes (Honninger et al. 2004a; Wagner et al. 2007) and a few for satellite validation (Brinkma et al. 2008; Irie et al. 2008; Wittrock et al. 2006; Fig. 7.11). The main difference between MAXDOAS and satellite measurements is the viewing geometry, which determines the vertical sensitivity of the measurements. As an example, while the sensitivity of a satellite UV/Vis measurement of  $\text{NO}_2$  decreases towards the surface over dark

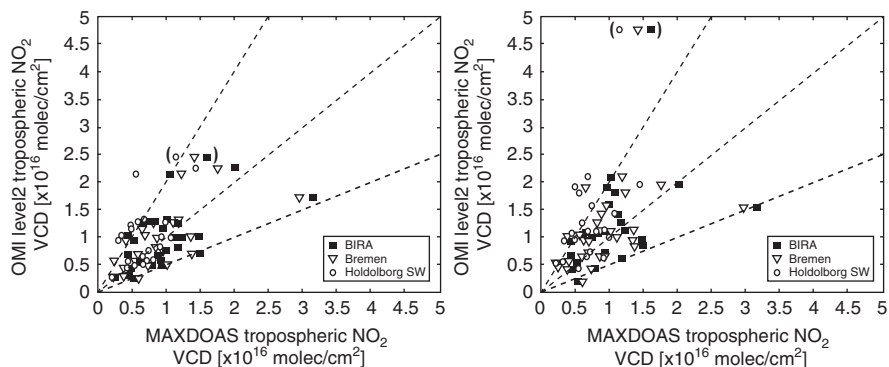


Fig. 7.11 Example of a recent study on satellite validation of tropospheric  $\text{NO}_2$ . OMI tropospheric  $\text{NO}_2$  from NASA, (version 1.0, left), and KNMI (DOMINO, right) for cloud fractions less than 20%, compared to those from three MAXDOAS instruments at Cabauw during the DANDELIONS campaign (from Brinkma et al. (2008)).

areas, the sensitivity of a MAXDOAS measurement decreases from the surface to the middle troposphere. Consequently, the tropospheric columns determined from the ground have a higher accuracy than the satellite measurements and depend much less on the *a priori* assumptions made in the retrieval. While the vertical integration problem can be solved by using ground-based remote sensing data, the complications from horizontal and temporal variability remain and have to be taken into account when selecting appropriate locations for validation.

## **b Fourier Transform Infrared Spectroscopy (FTIR)**

Many atmospheric trace species, including O<sub>3</sub>, NO<sub>2</sub>, N<sub>2</sub>O, CO, HNO<sub>3</sub>, CH<sub>4</sub>, exhibit absorption signatures in the infrared range. By the application of FTIR, the vertical column of these species can be detected with high-spectral-resolution measurements of solar spectrum absorption by the atmosphere (Chapter 3). If weather permits, FTIR can measure throughout the day, and observe the diurnal cycle of species such as NO<sub>2</sub> and HCHO. The need to observe the solar disc directly is a limiting feature. This is especially the case for instruments requiring manual intervention, at stations, which are frequently overcast, and at polar stations that experience polar night for several months of the year. In polar regions, the full moon can be used as infrared light source (Notholt et al. 1993). Water vapour (Schmid et al. 1996) and SO<sub>2</sub> (Mellqvist et al. 2005) are found mainly in the troposphere. Their column measurements can be used directly for tropospheric studies (Toon et al. 1989) and, if the comparison method handles appropriately spatial and temporal variability, they can be used directly for the validation of satellite tropospheric data products. For tropospheric species having a non-negligible stratospheric abundance, such as O<sub>3</sub>, N<sub>2</sub>O, CH<sub>4</sub> and HNO<sub>3</sub>, profiling techniques have been developed and validated against independent measurements (Pougatchev et al. 1995; 1996; Nakajima et al. 1997). It is interesting to note that nearly all FTIR stations are affiliated with the NDACC; consequently, the instruments and algorithms have to comply with rigorous validation protocols. For instance at the NDACC station Jungfraujoch in Switzerland, the FTIR column data record of CO, CH<sub>4</sub> and N<sub>2</sub>O extends back to the 1950s, from which secular trends have been calculated (Zander et al. 1989a; 1989b; 1994). FTIR measurements have been used successfully for the validation of SCIAMACHY CO, CH<sub>4</sub>, CO<sub>2</sub> and N<sub>2</sub>O columns (Dils et al. 2006). They have also been used for the validation of upper troposphere/lower stratosphere measurements by ENVISAT MIPAS (Cortesi et al. 2007; Ceccherini et al. 2008) and by SCISAT-1 ACE. Recent developments in ground-based FTIR include the retrieval of CO<sub>2</sub> (Yang et al. 2002), of SO<sub>2</sub> (Mellqvist et al. 2005), and of HCHO (Jones et al. 2009).

## **c Light Detection and Ranging (lidar)**

Information about the vertical distribution of several tropospheric species can be retrieved from lidar measurements. Aerosol profiles can be measured as backscatter

profiles, but for the retrieval of extinction, assumptions are needed about the backscatter to extinction ratio, the lidar ratio, as a function of height above the surface. Raman lidars, where Raman-shifted wavelengths for  $N_2$  or  $O_2$  are used, measure the extinction directly. Raman lidars are used in the EARLINET network. Vertical profiles of trace gases can be measured by DIAL systems. The elastic backscatter ratio by air is measured at several wavelengths where there are differences in the absorption by the target molecule (Measures 1992; Schouepnikoff et al. 1998). Applying a spectral analysis technique similar to DOAS, DIAL measurements yield the vertical distribution of  $O_3$  concentration and water vapour mixing ratio in the free troposphere (3 km to about 12 km at middle latitudes) with a temporal resolution of about 15 min and a vertical resolution of 50–300 m (Vogelmann and Trickl 2008). Unfortunately, the high sensitivity of the DIAL technique to aerosols and other effects limit its sensitivity and accuracy for gases in the PBL and its capacity to reach higher altitudes than those near the tropopause for  $O_3$ , and lower for  $H_2O$  and  $NO_2$ .

#### **d Sun Photometers**

Sun photometers are used to measure the column integrated atmospheric extinction, i.e. AOD (or Aerosol Optical Thickness – AOT). The AOD is the primary aerosol parameter retrieved from satellites. When AOD is available at several wavelengths, the Ångström exponent, describing the AOD wavelength dependence, can be derived. These parameters are available from sun photometer networks such as AERONET (Holben et al. 1998) and PHOTONS, which use CIMEL instruments, or the GAW PFR network that uses precision filter radiometers. AERONET provides additional aerosol parameters retrieved from Almuquantar scans. AERONET provides data every 15 min for cloud free conditions, in near real time (L1 and L1.5 products). The CIMEL instruments are calibrated each year and after calibration, the data are re-processed to provide L2 products. GAW PFR measures every minute but the products are not available in NRT.

### **7.5.3 Networks and Data Centres**

Many of the essential *in situ* and ground based measurements for air pollution and climate change (Essential Climate Variables, ECVs) contribute to long-term monitoring activities on national and international levels carried out under the auspices of WMO's GAW and GCOS. The use of these datasets gives long-term availability, traceability and known quality of the needed data. They have been acquired and checked following the defined QA/QC procedures of the respective networks and are usually publicly available through databases (Table 7.3). Additionally within EU framework programmes such as GEOMon (<http://www.geomon.eu>) or EUSAAR (<http://www.eusaar.net>), harmonized datasets of representative sites are provided on the European scale for selected parameters. An overview of databases and additional

**Table 7.6** Web sites listing validation activities and results

Instrument	website
SCIAMACHY	<a href="http://www.sciamachy.org/validation">http://www.sciamachy.org/validation</a>
OMI	<a href="http://www.knmi.nl/omi/research/validation">http://www.knmi.nl/omi/research/validation</a>
TES	<a href="http://tes.jpl.nasa.gov/data/validation">http://tes.jpl.nasa.gov/data/validation</a>
GOME-2	<a href="http://o3saf.fmi.fi/documents.html">http://o3saf.fmi.fi/documents.html</a>
MOPITT	<a href="http://mopitt.eos.ucar.edu/Validation">http://mopitt.eos.ucar.edu/Validation</a>

information about sites and measurement programmes are available on <http://www.gosic.org> or <http://gaw.empa.ch/gawsis> and data can be accessed through a large variety of data centres (Tables 7.3–7.5).

As geophysical validation of Earth Observation data remains a high priority, ESA has initiated a project to develop a Generic Environment for Calibration/validation Analysis (GECA), which is considered to become the next generation validation data centre. The evolution part of GECA is in the interoperability between various validation data centres through standardisation of metadata, and catalogue and data exchange. Currently data centre interoperability has started with the Aura Validation Data Centre (AVDC), ENVISAT Validation Data Centre (EVDC), EARLINET, GAW, GEOmon and NDACC.

#### 7.5.4 Validation Activities

As described in Section 7.3.1 each satellite instrument undergoes a planned validation phase, often including dedicated measurement campaigns. Table 7.6 lists a number of web sites where validation activities and results on tropospheric satellite products are archived. These web sites also contain additional documentation on validation strategies and requirements.

## 7.6 Future Validation strategies

### 7.6.1 Requirements for Future Validation Measurements

For the validation of tropospheric satellite products, a comprehensive set of correlative measurements is needed. These measurements should have ample coverage in space and time and in the range of values that can occur. In addition, they should be performed with a certain quality standard. The following general requirements can be formulated.

- Instruments for correlative measurements should ideally be placed in a global network and perform continuous measurements.
- A quality procedure, including regular intercomparisons, should be implemented in such a network.

- In choosing the sites for this network, it has to be considered that validation should be performed under various conditions (clean/polluted), but that the measurements should be representative for a larger area (i.e. a satellite ground pixel). This means that the surface height and albedo should not be too variable.
- The local variability for the measured species should be properly characterized or measured. This could mean that it is necessary to measure at various locations within a satellite pixel or in various directions (for remote sensing).
- A number of sites should have ample cloud-free conditions.
- Remote sensing measurements should be accompanied by *in situ* surface measurements.

Apart from the tropospheric species of interest, additional measurements should be made of aerosols, clouds, and boundary layer height.

### 7.6.2 Validation Strategy for Tropospheric O<sub>3</sub>

Currently, the main validation source for tropospheric O<sub>3</sub> is the ozone-sonde network. There is a need for more independent measurements to complement the ozone-sondes, preferably from a network of comparable instruments. The network should at least cover the tropics and northern mid-latitudes. Candidate instruments for such a network would be Brewer, MAXDOAS, and DIAL.

The DIAL tropospheric ozone lidar measures an O<sub>3</sub> profile in the free troposphere, but it needs to be complemented with additional boundary layer measurements. More DIAL instruments would be needed and they would need to be operated routinely. A Brewer network is already in place. It would be worthwhile to develop a retrieval algorithm for tropospheric O<sub>3</sub> from Brewers. In addition, MAXDOAS is a candidate for measuring tropospheric O<sub>3</sub>. A retrieval algorithm has to be developed and a network has to be set up.

In general, measurements should be done close to the satellite measuring time. Balloon, sonde and aircraft measurements, which often have constraints on the flight times, should be complemented with surface measurements and transport models with actual meteorological information to correct as much as possible for the inevitable time differences. Close to (precursor) emission sources, the collocation in time is even more important.

### 7.6.3 Validation Strategy for Tropospheric NO<sub>2</sub>

The only instruments currently measuring the tropospheric column of NO<sub>2</sub> are remote sensing instruments. *In situ* instruments have also been used in a few aircraft campaigns. The various remote sensing instruments have been developed relatively recently, and they still need thorough characterisation and validation. The current

accurate *in situ* instruments are rather heavy and are not suited for use on light aircrafts or small balloons.

A network of remote sensing instruments, complemented by *in situ* profiling techniques would be needed.

Light-weight/portable *in situ* measuring techniques should be developed so that sonde type measurements can be made in a network. The use of existing instruments such as (mini-)MAXDOAS and NO<sub>2</sub> lidar should be enhanced in existing networks such as NDACC. Further studies should assess the accuracy of these instruments.

Tropospheric NO<sub>2</sub> has a strong daily cycle, which makes the timing of validation measurements important. Since tropospheric NO<sub>2</sub> is so variable, the collocation with the satellite is critical. Also NO<sub>2</sub> has a high spatial variability. It is therefore important to place instruments in locations that are representative of the background concentration and not too close to the source. The most extensive campaign so far, focused on tropospheric NO<sub>2</sub> in particular, has been the CINDI campaign, June–July 2009, in Cabauw, The Netherlands (Fig. 7.12). Similar efforts should be encouraged in the future.



**Fig. 7.12** One of the more than 20 MAXDOAS-like instruments in use during the Cabauw Intercomparison campaign of nitrogen dioxide measuring instruments (CINDI), June–July 2009, Cabauw, The Netherlands.

### 7.6.4 Validation Strategy for CO

CO is measured at only a few sites, using flasks or continuous measurement methods (*in situ*; WMO-GAW 2010) and FTIR (remote sensing). FTIR measures total CO columns, given that CO is mostly in the troposphere, this approximates to tropospheric CO.

There is a small quasi-global network of ground-based FTIR instruments, but places with high CO emissions are not well covered, and the location of the FTIR instruments is often not ideal. Some FTIR instruments are situated too high and only measure part of the column, some are too close to the sea, where satellite measurements are inaccurate. The flask measurements from the Cooperative Air Sampling Network cover a wide region, but only give surface CO concentrations.

The FTIR network should be extended to optimize the coverage for CO validation. Large CO variability can be expected near source regions. There is a lack of CO column data over regions with high surface albedo.

The deployment of light instruments for sonde applications is highly recommended.

## References

- Alicke, B., U. Platt and J. Stutz, 2002, Impact of nitrous acid photolysis on the total hydroxyl radical budget during the Limitation of Oxidant Production/Pianura Padana Produzione di Ozone study in Milan, *J. Geophys. Res.*, **107**(D22), 8196, doi:10.1029/2000JD000075.
- Bergamaschi, P., C. Frankenberg, J.F. Meirink, M. Krol, F. Dentener, T. Wagner, U. Platt, J.O. Kaplan, S. Körner, M. Heimann, E.J. Dlugokencky and A. Goede, 2007, Satellite cartography of atmospheric methane from SCIAMACHY on board ENVISAT: 2. Evaluation based on inverse model simulations, *J. Geophys. Res.*, **112**, D02304, doi: 10.1029/2006JD007268.
- Blond, N., K.F. Boersma, H.J. Eskes, R.J. van der A, M. Van Roozendael, I. De Smedt, G. Bergametti and R. Vautard, 2007, Intercomparison of SCIAMACHY nitrogen dioxide observations, *in situ* measurements and air quality modeling results over Western Europe, *J. Geophys. Res.*, **112**, doi:10.1029/2006JD007277.
- Boersma, K.F., H.J. Eskes and E.J. Brinksma, 2004, Error analysis for tropospheric NO<sub>2</sub> retrieval from space, *J. Geophys. Res.*, **109**, D04311, doi:10.1029/2003JD003962.
- Boersma, K.F., D.J. Jacob, H.J. Eskes, R.W. Pinder, J. Wang and R.J. van der A, 2008, Intercomparison of SCIAMACHY and OMI tropospheric NO<sub>2</sub> columns: observing the diurnal evolution of chemistry and emissions from space, *J. Geophys. Res.*, **113**, 16S27, doi:10.1029/2007JD008832.
- Brinksma, E., G. Pinardi, R. Braak, H. Volten, A. Richter, A. Schönhardt, M. Van Roozendael, C. Fayt, C. Hermans, R. Dirksen, T. Vlemmix, A.J.C. Berkhout, D.P.J. Swart, H. Oetjen, F. Wittrock, T. Wagner, O.W. Ibrahim, G. de Leeuw, M. Moerman, L. Curier, E.A. Celarier, W.H. Knap, J.P. Veeffkind, H.J. Eskes, M. Allaart, R. Rothe, A.J.M. Pijters and P. Levelt, 2008, The 2005 and 2006 DANDELIONS NO<sub>2</sub> and Aerosol Intercomparison Campaigns, *J. Geophys. Res.*, **113**, 46, doi:10.1029/2007JD008808.
- Brewer, A.W., J.B. Kerr and C.T. McElroy, 1973, Nitrogen dioxide concentrations in the atmosphere, *Nature*, **246**, 129–133.
- Buchwitz, M., R. de Beek, S. Noël, J.P. Burrows, H. Bovensmann, O. Schneising, I. Khlystova, M. Bruns, H. Bremer, P. Bergamaschi, S. Körner and M. Heimann, 2006, Atmospheric carbon

- gases retrieved from SCIAMACHY by WFM-DOAS: version 0.5 CO and CH<sub>4</sub> and impact of calibration improvements on CO<sub>2</sub> retrieval, *Atmos. Chem. Phys.*, **6**, 2727–2751.
- Buchwitz, M., I. Khlystova, H. Bovensmann and J.P. Burrows, 2007, Three years of global carbon monoxide from SCIAMACHY: comparison with MOPITT and first results related to the detection of enhanced CO over cities, *Atmos. Chem. Phys.*, **7**, 2399–2411.
- Bucsela, E.J., A.E. Perring, R.C. Cohen, K.F. Boersma, E.A. Celarier, J.F. Gleason, M.O. Wenig, T.H. Bertram, P.J. Wooldridge, R. Dirksen and J.P. Veefkind, 2008, Comparison of tropospheric NO<sub>2</sub> from *in situ* aircraft measurements with near-real-time and standard product data from OMI, *J. Geophys. Res.*, **113**, D16S31, doi:10.1029/2007JD008838.
- Calisesi, Y., V.T. Soebijanta and R. van Oss, 2005, Regridding of remote soundings: Formulation and application to ozone profile comparison, *J. Geophys. Res.*, **110**, D23306, doi:10.1029/2005JD006122.
- Ceccherini, S., U. Cortesi, P.T. Verronen and E. Kyrölä, 2008, Technical Note: Continuity of MIPAS-ENVISAT operational ozone data quality from full- to reduced-spectral-resolution operation mode, *Atmos. Chem. Phys.*, **8**, 2201–2212.
- Celarier, E.A., E.J. Brinksma, J.F. Gleason, J.P. Veefkind, A. Cede, J.R. Herman, D. Ionov, F. Goutail, J.-P. Pommereau, J.-C. Lambert, M. van Roozendaal, G. Pinardi, F. Wittrock, A. Schönhardt, A. Richter, O.W. Ibrahim, T. Wagner, B. Bojkov, G. Mount, E. Spinei, C.M. Chen, T.J. Pongetti, S.P. Sander, E.J. Bucsela, M.O. Wenig, D.P.J. Swart, H. Volten, M. Kroon and P.F. Levelt, 2008, Validation of Ozone Monitoring Instrument nitrogen dioxide columns, *J. Geophys. Res.*, **113**, D15S15, doi:10.1029/2007JD008908.
- Cleary, P.A., P.J. Wooldridge and R.C. Cohen, 2002, Laser-induced fluorescence detection of atmospheric NO<sub>2</sub> with a commercial diode laser and a supersonic expansion, *Appl. Optics*, **41**, 6950–6956.
- Cortesi, U., J.C. Lambert, C. De Clercq, G. Bianchini, T. Blumenstock, A. Bracher, E. Castelli, V. Catoire, K.V. Chance, M. De Mazière, P. Demoulin, S. Godin-Beekmann, N. Jones, K. Jucks, C. Keim, T. Kerzenmacher, H. Kuellmann, J. Kuttippurath, M. Iarlori, G.Y. Liu, Y. Liu, I.S. McDermid, Y.J. Meijer, F. Mencaraglia, S. Mikuteit, H. Oelhaf, C. Piccolo, M. Pirre, P. Raspollini, F. Ravagnani, W.J. Reburn, G. Redaelli, J.J. Remedios, H. Sembhi, D. Smale, T. Steck, A. Taddei, C. Varotsos, C. Vigouroux, A. Waterfall, G. Wetzel and S. Wood, 2007, Geophysical validation of MIPAS-ENVISAT operational ozone data, *Atmos. Chem. Phys.*, **7**, 4807–4867.
- Day, D.A., M.B. Dillon, P.J. Wooldridge, J.A. Thornton, R.S. Rosen, E.C. Wood, and R.C. Cohen, 2003, On alkyl nitrates, O<sub>3</sub>, and the “missing NO<sub>y</sub>”, *J. Geophys. Res.*, **108(D16)**, 4501, doi:10.1029/2003JD003685.
- de Laat, A.T.J., A.M.S. Gloudemans, I. Aben, M. Krol, J.F. Meirink, G.R. van der Werf and H. Schrijver, 2007, Scanning Imaging Absorption Spectrometer for Atmospheric Cartography carbon monoxide total columns: Statistical evaluation and comparison with chemistry transport model results, *J. Geophys. Res.*, **112**, doi:10.1029/2006JD008256.
- de Laat, A. T. J., A. M. S. Gloudemans, I. Aben, and H. Schrijver, 2010, Global evaluation of SCIAMACHY and MOPITT carbon monoxide column differences for 2004–2005, *J. Geophys. Res.*, **115**, D06307, doi:10.1029/2009JD012698.
- De Smedt, I., J.-F. Müller, T. Stavrou, R. van der A, H. Eskes and M. Van Roozendaal, 2008, Twelve years of global observations of formaldehyde in the troposphere using GOME and SCIAMACHY sensors, *Atmos. Chem. Phys.*, **8**, 4947–4963.
- Dils, B., M. De Mazière, J.F. Müller, T. Blumenstock, M. Buchwitz, R. de Beek, P. Demoulin, P. Duchatelet, H. Fast, C. Frankenberg, A. Gloudemans, D. Griffith, N. Jones, T. Kerzenmacher, I. Kramer, E. Mahieu, J. Mellqvist, R.L. Mittermeier, J. Notholt, C.P. Rinsland, H. Schrijver, D. Smale, A. Strandberg, A.G. Straume, W. Stremme, K. Strong, R. Sussmann, J. Taylor, M. van den Broek, V. Velasco, T. Wagner, T. Warneke, A. Wiacek and S. Wood, 2006, Comparisons between SCIAMACHY and ground-based FTIR data for total columns of CO, CH<sub>4</sub>, CO<sub>2</sub> and N<sub>2</sub>O, *Atmos. Chem. Phys.*, **6**, 1953–1976.
- Dobber M., Q. Kleipool, R. Dirksen, P. Levelt, G. Jaross, S. Taylor, T. Kelly, L. Flynn, G. Lempelmeier, N. Rozemeijer, 2008, Validation of Ozone Monitoring Instrument level 1b data products, *J. Geophys. Res.*, **113**, D15S06, doi:10.1029/2007JD008665.

- Dobson, G.M.B. and D.N. Harrison, 1926, Measurements of the amount of ozone in the Earth's Atmosphere and its Relation to other Geophysical Conditions, *Proc. R. Soc. London*, **110**, 660–693.
- Dorf, M., H. Bösch, A. Butz, C. Camy-Peyret, M.P. Chipperfield, A. Engel, F. Goutail, K. Grunow, F. Hendrick, S. Hrechanyy, B. Naujokat, J.-P. Pommereau, M. Van Roozendael, C. Sioris, F. Stroh, F. Weidner, and K. Pfeilsticker, 2006, Balloon-borne stratospheric BrO measurements: comparison with Envisat/SCIAMACHY BrO limb profiles, *Atmos. Chem. Phys.*, **6**, 2483–2501.
- Eck, T.F., B.N. Holben, J.S. Reid, O. Dubovik, A. Smirnov, N.T. O'Neill, I. Slutsker and S. Kinne, 1999, Wavelength dependence of the optical depth of biomass burning, urban and desert dust aerosols, *J. Geophys. Res.*, **104**, 31333–31350.
- Emmons, L.K., D.P. Edwards, M.N. Deeter, J.C. Gille, T. Campos, P. Nédélec, P. Novelli and G. Sachse, 2009, Measurements of Pollution In The Troposphere (MOPITT) validation through 2006, *Atmos. Chem. Phys.*, **9**, 1795–1803.
- Eskes, H.J., P.F.J. van Velthoven, P.J.M. Valks and H.M. Kelder, 2003, Assimilation of GOME total-ozone satellite observations in a three-dimensional tracer-transport model, *Q. J. R. Met. Soc.*, **129**, 1663–1681, doi: 10.1256/qj.02.14.
- Ganzeveld, L. and J. Lelieveld, 1995, Dry deposition parameterization in a chemistry general circulation model and its influence on the distribution of reactive trace gases, *J. Geophys. Res.*, **100(10)**, 20999–21012.
- Hagolle, O., Ph. Goloub, P.Y. Deschamps, H. Cosnefroy, X. Briottet, T. Bailleur, J.M. Nicolas, F. Parol, B. Lafrance and M. Herman, 1999, Results of POLDER in-flight calibration, *IEEE Transactions on Geoscience and Remote Sensing*, **37**, 03.
- Heckel, A., A. Richter, T. Tarsu, F. Wittrock, C. Hak, I. Pundt, W. Junkermann and J.P. Burrows, 2005, MAX-DOAS measurements of formaldehyde in the Po-Valley, *Atmos. Chem. Phys.*, **5**, 909–918.
- Heland, J., H. Schlager, A. Richter and J.P. Burrows, 2002, First comparison of tropospheric NO<sub>2</sub> column densities retrieved from GOME measurements and *in situ* aircraft profile measurements, *Geophys. Res. Lett.*, **29(20)**, 1983.
- Holben, B. N., T.F. Eck, I. Slutsker, D. Tanré, J.P. Buis, A. Setzer, E. Vermote, J.A. Reagan, Y.J. Kaufman, T. Nakajima, F. Lavenu, I. Jankowiak and A. Smirnov, 1998, AERONET - A federated instrument network and data archive for aerosol characterization, *Remote Sens. Environ.*, **66(1)**, 1–16.
- Holton, J.R., P.H. Haynes, M.E. McIntyre, A.R. Douglas, R.B. Rood and L. Pfister, 1995, Stratosphere-troposphere exchange, *Rev. Geophys.*, **33**, 403 – 439.
- Hönninger G. and U. Platt, 2002, The Role of BrO and its Vertical Distribution during Surface Ozone Depletion at Alert, *Atmos. Environ.*, **36**, 2481–2489.
- Hönninger, G., H. Leser, O. Sebastián and U. Platt, 2004a, Ground-based measurements of halogen oxides at the Hudson Bay by active longpath DOAS and passive MAX-DOAS, *Geophys. Res. Lett.*, **31**, L04111, doi:10.1029/2003GL018982.
- Hönninger, G., C. von Friedeburg and U. Platt, 2004b, Multi axis differential optical absorption spectroscopy (MAX-DOAS), *Atmos. Chem. Phys.*, **4**, 231–254.
- Irie, H., Y. Kanaya, H. Akimoto, H. Iwabuchi, A. Shimizu, and K. Aoki, 2008, First retrieval of tropospheric aerosol profiles using MAX-DOAS and comparison with lidar and sky radiometer measurements, *Atmos. Chem. Phys.*, **8(2)**, 341–350.
- ISO/IEC Guide 99-12: 2007 International Vocabulary of Metrology – Basic and General Concepts and Associated Terms, VIM.
- Jaross G. and J. Warner, 2008, Use of Antarctica for validating reflected solar radiation measured by satellite sensors, *J. Geophys. Res.*, **113**, D16S34, doi:10.1029/2007JD008835.
- Jones, N.B., K. Riedel, W. Allan, S. Wood, P.L. Palmer, K. Chance and J. Notholt, 2009, Long-term tropospheric formaldehyde concentrations deduced from ground-based fourier transform solar infrared measurements, *Atmos. Chem. Phys.*, **9**, 7131–7142.
- Kahn, R. A., W.-H. Li, C. Moroney, D. J. Diner, J. V. Martonchik and E. Fishbein, 2007, Aerosol source plume physical characteristics from space-based multiangle imaging, *J. Geophys. Res.*, **112**, D11205, doi:10.1029/2006JD007647.

- Kebabian, P.L., S.C. Herndon and A. Freedman, 2005, Detection of nitrogen dioxide by cavity attenuated phase shift spectroscopy, *Anal. Chem.*, **77**, 724–728.
- Kelly, T.J., C.W. Spicer and G.F. Ward, 1990, An assessment of the luminol chemiluminescence technique for measurements of NO<sub>2</sub> in ambient air, *Atmos. Environ.*, **24A**, 2397–2403.
- Klausen, J., C. Zellweger, B. Buchmann and P. Hofer, 2003, Uncertainty and bias of surface ozone measurements at selected Global Atmosphere Watch sites, *J. Geophys. Res.*, **108**, 4622, doi:10.1029/2003JD003710.
- Kleipool, Q.L., M.R. Dobber, J.F. de Haan, and P.F. Levelt, 2008, Earth surface reflectance climatology from 3 years of OMI data, *J. Geophys. Res.*, **113**, doi:10.1029/2008JD010290.
- Koelemeijer, R., P. Stammes, J. Hovenier and J. de Haan, 2001, A fast method for retrieval of cloud parameters using oxygen A band measurements from the Global Ozone Monitoring Experiment, *J. Geophys. Res.*, **106**(4), 3475–3490.
- Koelemeijer, R.B.A., J.F. de Haan and P. Stammes, 2003, A Database of spectral surface reflectivity in the range 335 - 772 nm derived from 5.5 years GOME observations, *J. Geophys. Res.*, **108**, 4070, doi:10.1029/2002JD002429.
- Konovalov, I.B., M. Beekman, J.P. Burrows and A. Richter, 2008, Satellite measurement based estimates of decadal changes in European nitrogen oxides emissions, *Atmos. Chem. Phys.*, **8**, 2723–2641.
- Kramer, L.J., R.J. Leigh, J.J. Remedios, and P.S. Monks, 2008, Comparison of OMI and ground-based *in situ* and MAX-DOAS measurements of tropospheric nitrogen dioxide in an urban area, *J. Geophys. Res.*, **113**, D16S39, doi:10.1029/2007JD009168.
- Kroon M., J.P. Veefkind, M. Sneep, R.D. McPeters, P.K. Bhartia and P.F. Levelt, 2008, Comparing OMI-TOMS and OMI-DOAS total ozone column data, *J. Geophys. Res.*, **113**, D16S28, doi:10.1029/2007JD008798.
- Krotkov, N.A., B. McClure, R.R. Dickerson, S.A. Carn, C. Li, P.K. Bhartia, K. Yang, A.J. Krueger, Z. Li, P.F. Levelt, H. Chen, P. Wang and D. Lu, 2008, Validation of SO<sub>2</sub> retrievals from the Ozone Monitoring Instrument over NE China, *J. Geophys. Res.*, **113**, 40, doi:10.1029/2007JD008818.
- Lamsal L.N., R.V. Martin, A. van Donkelaar, M. Steinbacher, E.A. Celarier, E. Bucsela, E.J. Dunlea and J.P. Pinto, 2008, Ground-level nitrogen dioxide concentrations inferred from the satellite-borne Ozone Monitoring Instrument, *J. Geophys. Res.*, **113**, D16308, doi:10.1029/2007JD009235.
- Lauer, A., M. Dameris, A. Richter, and J.P. Burrows, 2002, Tropospheric NO<sub>2</sub> columns: a comparison between model and retrieved data from GOME measurements, *Atmos. Chem. Phys.*, **2**, 67–78.
- Leigh, R.J., G.K. Corlett, U. Friess and P.S. Monks, 2006, Concurrent multiaxis differential optical absorption spectroscopy system for the measurement of tropospheric nitrogen dioxide, *Appl. Optics*, **45**(28), 7504–7518.
- Li, Y.Q., K.L. Demerjian, M.S. Zahniser, D.D. Nelson, J.B. McManus and S.C. Herndon, 2004, Measurement of formaldehyde, nitrogen dioxide, and sulfur dioxide at Whiteface Mountain using a dual tunable diode laser system, *J. Geophys. Res.*, **109**, D16S08, doi:10.1029/2003JD004091.
- Martin, R.V., D.J. Jacob, K. Chance, T.P. Kurosu, P.I. Palmer and M.J. Evans, 2003, Global inventory of nitrogen oxide emissions constrained by space-based observations of NO<sub>2</sub> columns, *J. Geophys. Res.*, **108**, doi:10.1029/2003JD003453.
- Matsumoto, J., J. Hirokawa, H. Akimoto and Y. Kajii, 2001, Direct measurement of NO<sub>2</sub> in the marine atmosphere by laser-induced fluorescence technique, *Atmos. Environ.*, **35**, 2803–2814, doi:10.1016/S1352-2310(01)00078-4.
- McKenzie, R.L. and P.V. Johnston, 1982, Seasonal variation in stratospheric NO<sub>2</sub> at 45 degrees S, *Geophys. Res. Lett.*, **9**, 1255–1258.
- Measures, R.M., 1992, *Laser Remote Sensing. Fundamentals and Applications*, Krieger, New-York, pp 510.

- Mellqvist, J., B. Galle, M. Kihlman and M. Burton, 2005, Mobile solar FTIR measurements of SO<sub>2</sub> and halogens in the gas plumes of active volcanoes, *Geophys. Res. Abstracts*, **7**, 08987.
- Müller, J.-F. and T. Stavrou, 2005, Inversion of CO and NO<sub>x</sub> emissions using the adjoint of the IMAGES model, *Atmos. Chem. Phys.*, **4**, 1157–1186.
- Murphy, J.G., D.A. Day, P.A. Cleary, P.J. Wooldridge and R.C. Cohen, 2006, Observations of the diurnal and seasonal trends in nitrogen oxides in the western Sierra Nevada, *Atmos. Chem. Phys.*, **6**, 5321–5338.
- Nakajima, H., X. Liu, I. Murata, Y. Kondo, F.J. Murcray, M. Koike, Y. Zhao and H. Nakane, 1997, Retrieval of vertical profiles of ozone from high resolution infrared solar spectra at Rikubetsu, Japan, *J. Geophys. Res.*, **102**, 29981–29990.
- Nassar, R., J.A. Logan, H.M. Worden, I.A. Megretskaia, K.W. Bowman, G.B. Osterman, A.M. Thompson, D.W. Tarasick, S. Austin, H. Claude, M.K. Dubey, W.K. Hocking, B.J. Johnson, E. Joseph, J. Merrill, G.A. Morris, M. Newchurch, S.J. Oltmans, F. Posny, F.J. Schmidlin, H. Vömel, D.N. Whiteman and J.C. Witte, 2008, Validation of Tropospheric Emission Spectrometer (TES) nadir ozone profiles using ozonesonde measurements, *J. Geophys. Res.*, **113**, D15S17, doi:10.1029/2007JD008819.
- Noel, S., M. Buchwitz, H. Bovensmann and J.P. Burrows, 2005, Validation of SCIAMACHY AMC-DOAS water vapour columns, *Atmos. Chem. Phys.*, **5**, 1835–1841.
- Notholt, J., R. Neuber, O. Schrems and T. von Clarmann, 1993, Stratospheric trace gas concentrations in the Arctic polar night derived by FTIR-spectroscopy with the moon as IR light source, *Geophys. Res. Lett.*, **20**, 2059–2062.
- Noxon, J. F., 1975, Nitrogen Dioxide in the Stratosphere and Troposphere measured by Ground-based Absorption Spectroscopy, *Science*, **189**, 547–549.
- Ordoñez, C., A. Richter, M. Steinbacher, C. Zellweger, H. Nüss, J.P. Burrows and A.S.H. Prévôt, 2006, Comparison of 7 years of satellite-borne and ground-based tropospheric NO<sub>2</sub> measurements around Milan, Italy, *J. Geophys. Res.*, **111**, doi:10.1029/2005JD006305.
- Osthoff, H.D., S.S. Brown, T.B. Ryerson, T.J. Fortin, B.M. Lerner, E.J. Williams, A. Pettersson, T. Baynard, W.P. Dubé, S.J. Ciciora and A.R. Ravishankara, 2006, Measurement of atmospheric NO<sub>2</sub> by pulsed cavity ring-down spectroscopy, *J. Geophys. Res.*, **111**, D12305, doi:10.1029/2005JD006942.
- Platt, U. and D. Perner, 1980, Direct measurements of atmospheric CH<sub>2</sub>O, HNO<sub>2</sub>, NO<sub>2</sub>, and SO<sub>2</sub> by differential optical absorption in the near UV, *J. Geophys. Res. Oceans*, **85**, 7453–7458.
- Pommereau, J.P. and F. Goutail, 1988a, O<sub>3</sub> and NO<sub>2</sub> Ground-Based Measurements by Visible Spectrometry during Arctic Winter and Spring 1988, *Geophys. Res. Lett.*, **15**, 891.
- Pommereau, J.P. and F. Goutail, 1988b, Stratospheric O<sub>3</sub> and NO<sub>2</sub> Observations at the Southern Polar Circle in Summer and Fall 1988, *Geophys. Res. Lett.*, **15**, 895.
- Pougatchev, N.S., B.J. Connor, and C.P. Rinsland, 1995, Infrared measurements of the ozone vertical distribution above Kitt Peak, *J. Geophys. Res.*, **100**, 16689–16698.
- Pougatchev, N.S., B.J. Connor, N.B. Jones, C.P. Rinsland, 1996, Validation of ozone profile retrievals from infrared ground-based solar spectra, *Geophys. Res. Lett.*, **23**(13), 1637–1640.
- Remer, L. A., Y. J. Kaufman, D. Tanré, S. Mattoo, D. A. Chu, J. V. Martins, R-R. Li, C. Ichoku, R. C. Levy, R. G. Kleidman, T. F. Eck, E. Vermote and B. N. Holben, 2005, The MODIS aerosol algorithm, products, and validation, *J. Atmos. Sci.*, **62**(4), 947–973.
- Richter, A., J. Leitão, A. Heckel and J.P. Burrows, 2007, Synergistic use of multiple sensors for tropospheric NO<sub>2</sub> measurements, Presentation at the ACCENT AT2 workshop “Tropospheric NO<sub>2</sub> measured by satellites”, 10–12 Sept 2007, KNMI, De Bilt, The Netherlands.
- Robles-Gonzalez, C., G. de Leeuw, R. Decae, J. Kusmierczyk-Michulec and P. Stammes, 2006, Aerosol properties over the Indian Ocean Experiment (INDOEX) campaign area retrieved from ATSR-2, *J. Geophys. Res.*, **111**, D15205, doi:10.1029/2005JD006184.
- Rodgers, C.D. and B.J. Connor, Intercomparison of remote sounding instruments, 2003, *J. Geophys. Res.*, **108** (D3), 4116, doi:10.1029/2002JD002299.

- Roelofs G. J., A.S. Kentarchos, T. Trickl, A. Stohl, W.J. Collins, R.A. Crowther, D. Hauglustaine, A. Klonecki, K.S. Law, M.G. Lawrence, R. von Kuhlmann and M. van Weele, 2003 Intercomparison of tropospheric ozone models: Ozone transport in a complex tropopause folding event, *J. Geophys. Res.*, **108** (12), 8529, doi:10.1029/2003JD003462.
- Sanders, R.W., S. Solomon, J.P. Smith, L. Perliski, H.L. Miller, G.H. Mount, J.G. Keys and A.L. Schmeltekopf, 1993, Visible and Near-Ultraviolet Spectroscopy at McMurdo Station Antarctica, 9. Observations of OCIO from April to October 1991, *J. Geophys. Res.*, **98**(D4), 7219–7228.
- Schaap, M., A. Apituley, R.M.A. Timmermans, R.B.A. Koelemeijer and G. de Leeuw, 2009, Exploring the relation between aerosol optical depth and PM<sub>2.5</sub> at Cabauw, the Netherlands, *Atmos. Chem. Phys.*, **9**, 909–925.
- Schaub, D., K.F. Boersma, J.W. Kaiser, A.K. Weiss, D. Folini, H.J. Eskes and B. Buchmann, 2006, Comparison of GOME tropospheric NO<sub>2</sub> columns with NO<sub>2</sub> profiles deduced from ground-based *in situ* measurements, *Atmos. Chem. Phys.*, **6**, 3211–3229.
- Schaub, D., D. Brunner, K.F. Boersma, J. Keller, D. Folini, B. Buchmann, H. Berresheim and J. Staehelin, 2007, SCIAMACHY tropospheric NO<sub>2</sub> over Switzerland: estimates of NO<sub>x</sub> lifetimes and impact of the complex Alpine topography on the retrieval, *Atmos. Chem. Phys.*, **7**, 5971–5987.
- Schmid, B., K.J. Thome, Ph. Demoulin, R. Peter, C. Matzler and J. Sekler, 1996, Comparison of modeled and empirical approaches for retrieving columnar water vapor from solar transmittance measurements in the 0.94 micron region, *J. Geophys. Res.*, **101**, 9345–9358.
- Schoulepnikoff, L., H. van den Bergh, V. Mitev and B. Calpini, 1998, Tropospheric air pollution monitoring lidar, in: Meyers, R.A. (editor), *The Encyclopedia of Environmental Analysis and Remediation*, John Wiley and Sons, New York, 4873–4909.
- Schutgens, N.A.J. and P. Stammes, 2003, A novel approach to the polarization correction of spaceborne spectrometers, *J. Geophys. Res.*, **108** (D7), 4229, doi:10.1029/2002JD002736.
- Schutgens, N.A.J., L.J. Tilstra, P. Stammes and F.-M. Bréon, 2004, On the relationship between Stokes parameters Q and U of atmospheric ultraviolet/visible/near-infrared radiation, *J. Geophys. Res.*, **109**, D09205, doi:10.1029/2003JD004081.
- Shindell, D.T., G. Faluvegi and L.K. Emmons, 2005, Inferring carbon monoxide pollution changes from space-based observations, *J. Geophys. Res.*, **110**, doi:10.1029/2005JD006132.
- Sinreich, R., U. Frieb, T. Wagner and U. Platt, 2005, Multi axis differential optical absorption spectroscopy (MAXDOAS) of gas and aerosol distributions, *Faraday Discuss.*, **130**, 153–164, doi:10.1039/B419274P.
- Sneep, M., R. Braak, E. Brinksma and M. Kroon, 2006, Documentation for the ‘CAMA’ verification and validation toolkit, Version 1.2, MA-OMIE-KNMI-832, KNMI, De Bilt, The Netherlands.
- Sneep M., J.F. de Haan, P. Stammes, P. Wang, C. Vanbauce, J. Joiner, A.P. Vasilkov and P.F. Levelt, 2008, Three-way comparison between OMI and PARASOL cloud pressure products, *J. Geophys. Res.*, **113**, D15S23, doi:10.1029/2007JD008694.
- Solomon, S., A.L. Schmeltekopf and R.W. Sanders, 1987, On the interpretation of zenith sky absorption measurements, *J. Geophys. Res.*, **92**, 8311–8319.
- Stammes P., M. Sneep, J.F. de Haan, J.P. Veefkind, P. Wang, P.F. Levelt, 2008, Effective cloud fractions from the Ozone Monitoring Instrument: Theoretical framework and validation, *J. Geophys. Res.*, **113**, D16S38, doi:10.1029/2007JD008820.
- Steinbacher, M., C. Zellweger, B. Schwarzenbach, S. Bugmann, B. Buchmann, C. Ordóñez, A.S. H. Prevot and C. Hueglin, 2007, Nitrogen oxide measurements at rural sites in Switzerland: Bias of conventional measurement techniques, *J. Geophys. Res.*, **112**, D11307, doi:10.1029/2006JD007971.
- Sussmann, R. and M. Buchwitz, 2005, Initial validation of ENVISAT/SCIAMACHY columnar CO by FTIR profile retrievals at the Ground-Truthing Station Zugspitze, *Atmos. Chem. Phys.*, **5**, 1497–1503.

- Theys, N., F. Hendrick, M. Van Roozendael, I. De Smedt, C. Fayt and R. van der A, 2006, Retrieval of BrO Columns from SCIAMACHY and their Validation Using Ground-Based DOAS Measurements, *Proc. of the First Atmospheric Science Conference*, ESRIN, Frascati, Italy, 8 – 12 May 2006, ESA SP-628.
- Tilstra L.G., G. van Soest, P. Stammes, 2005, Method for in-flight satellite calibration in the ultraviolet using radiative transfer calculations, with application to Scanning Imaging Absorption Spectrometer for Atmospheric Cartography (SCIAMACHY), *J. Geophys. Res.*, **110**, D18311, doi:10.1029/2005JD005853.
- Tilstra L.G. and P. Stammes, 2007, Earth reflectance and polarization intercomparison between SCIAMACHY onboard Envisat and POLDER onboard ADEOS-2, *J. Geophys. Res.*, **112**, D11304, doi:10.1029/2006JD007713.
- Toon, G.C., C.B. Farmer, P.W. Schaper, J.-F. Blavier and L.L. Lowes, 1989, Ground-based Infrared Measurements of Tropospheric Source Gases over Antarctica during the 1986 Austral Spring, *J. Geophys. Res.*, **94**, 11613–11624.
- van Noije, T.P.C., H.J. Eskes, F.J. Dentener, D.S. Stevenson, K. Ellingsen, M.G. Schultz, O. Wild, M. Amann, C.S. Atherton, D.J. Bergmann, I. Bey, K.F. Boersma, T. Butler, J. Cofala, J. Drevet, A.M. Fiore, M. Gauss, D.A. Hauglustaine, L.W. Horowitz, I.S.A. Isaksen, M.C. Krol, J.-F. Lamarque, M.G. Lawrence, R.V. Martin, V. Montanaro, J.-F. Müller, G. Pitari, M.J. Prather, J. A. Pyle, A. Richter, J.M. Rodriguez, N.H. Savage, S.E. Strahan, K. Sudo, S. Szopa and M. Van Roozendael, 2006, Multi-model ensemble simulations of tropospheric NO<sub>2</sub> compared with GOME retrievals for the year 2000, *Atmos. Chem. Phys.*, **6**, 2943–2979.
- van Diedenhoven B., O.P. Hasekamp, J. Landgraf, 2007, Retrieval of cloud parameters from satellite-based reflectance measurements in the ultraviolet and the oxygen A-band, *J. Geophys. Res.*, **112**, D15208, doi:10.1029/2006JD008155.
- Van Roozendael, M., D. Loyola, R. Spurr, D. Balis, J.-C. Lambert, Y. Livschitz, T. Ruppert, P. Valks, P. Kenter, C. Fayt and C. Zehner, 2006, Ten years of GOME/ERS-2 total ozone data – The new GOME Data Processor (GDP) Version 4: I Algorithm Description, *J. Geophys. Res.*, **111**, D14311, doi:10.1029/2005JD006375.
- Veeffkind, J.P. and J.F. de Haan, 2001, DOAS Total Ozone Algorithm, in Barthia, P.K. (editor), *OMI Algorithm Theoretical Basis Document*, Volume II – Chapter 3, ATBD-OMI-02, Version 1.0
- Velders, G.J., C. Granier, R.W. Portmann, K. Pfeilsticker, M. Wenig, T. Wagner, U. Platt, A. Richter, and J.P. Burrows, 2001, Global tropospheric NO<sub>2</sub> column distributions: Comparing three-dimensional model calculations with GOME measurements, *J. Geophys. Res.*, **106**, 12643–12660.
- Vogelmann, H. and T. Trickl, 2008, Wide-range sounding of free-tropospheric water vapor with a differential-absorption lidar (DIAL) at a high-altitude station, *Appl. Optics*, **47**, 2116–2132.
- Wagner, T., O. Ibrahim, R. Sinreich, U. Frieß, R. von Glasow and U. Platt, 2007, Enhanced tropospheric BrO over Antarctic sea ice in mid winter observed by MAX-DOAS on board the research vessel Polarstern, *Atmos. Chem. Phys.*, **7**(12), 3129–3142.
- Wang, P., P. Stammes, R. van der A, G. Pinardi and M. VanRoozendael, 2008, FRESCO+: an improved O<sub>2</sub> A-band cloud retrieval algorithm for tropospheric trace gas retrievals, *Atmos. Chem. Phys.*, **8**, 6565–6576.
- Wittrock, F., H. Oetjen, A. Richter, S. Fietkau, T. Medeke, A. Rozanov and J.P. Burrows, 2004, MAX-DOAS measurements of atmospheric trace gases in Ny-Alesund - Radiative transfer studies and their application, *Atmos. Chem. Phys.*, **4**, 955–966.
- Wittrock, F., A. Richter, H. Oetjen, J.P. Burrows, M. Kanakidou, S. Myriokefalitakis, R. Volkamer, S. Beirle, U. Platt and T. Wagner, 2006, Simultaneous global observations of glyoxal and formaldehyde from space, *Geophys. Res. Lett.*, **33**, L16804, doi:10.1029/2006GL026310.
- WMO-GAW Report No. 192, 2010, Guidelines for the Measurement of Atmospheric Carbon Monoxide, WMO/TD-No. 1551.

- Yang, A., G.C. Toon, J.S. Margolis and P.O. Wennberg, 2002, Atmospheric CO<sub>2</sub> retrieved from ground-based near IR spectra, *Geophys. Res. Lett.*, **29**(9), doi: 10.1029/2001GL014537.
- Yudin, V.A., G. Pétron, J.-F. Lamarque, B.V. Khattatov, P.G. Hess, L.V. Lyjak, J.C. Gille, D.P. Edwards, M.N. Deeter and L.K. Emmons, 2004, Assimilation of the 2000–2001 CO MOPITT retrievals with optimized surface emissions, *Geophys. Res. Lett.*, **31**, doi:10.1029/2004GL021037.
- Zander, R., Ph. Demoulin, D.H. Ehhalt, U. Schmidt and C.P. Rinsland, 1989a, Secular increase of the total vertical column abundance of carbon monoxide above central Europe since 1950, *J. Geophys. Res.*, **94**, 11020–11028.
- Zander, R., Ph. Demoulin, D.H. Ehhalt and U. Schmidt, 1989b, Secular increase of the vertical column abundance of methane derived from IR solar spectra recorded at the Jungfraujoch station, *J. Geophys. Res.*, **94**, 11029–11039.
- Zander, R., D.H. Ehhalt, C.P. Rinsland, U. Schmidt, E. Mahieu, J. Rudolph, P. Demoulin, G. Roland, L. Delbouille and A.J. Sauval, 1994, Secular trend and seasonal variability of N<sub>2</sub>O above the Jungfraujoch station determined from IR solar spectra, *J. Geophys. Res.*, **99**, 16745–16756.
- Zellweger C., C. Hüglin, J. Klausen, M. Steinbacher, M. Vollmer and B. Buchmann, 2009, Inter-comparison of four different carbon monoxide measurement techniques and evaluation of the long-term carbon monoxide time series of Jungfraujoch, *Atmos. Chem. Phys.*, **9**, 3491–3503.
- Zhou, Y., D. Brunner, K.F. Boersma, R. Dirksen and P. Wang, 2009, An improved tropospheric NO<sub>2</sub> retrieval for OMI observations in the vicinity of mountainous terrain, *Atmos. Meas. Tech.*, **2**(2), 401–416